EVALUATING THE CORRELATION CHARACTERISTICS
OF ARBITRARY AM AND FM RADIO SIGNALS
FOR THE PURPOSE OF NAVIGATION

THESIS

Bryan S. Kim, Second Lieutenant, USAF

AFIT/GE/ENG/06-28

AFIT/GE/ENG/06-28

EVALUATING THE CORRELATION CHARACTERISTICS OF ARBITRARY AM AND FM RADIO SIGNALS FOR THE PURPOSE OF NAVIGATION

THESIS

Presented to the Faculty

Department of Electrical and Computer Engineering

Graduate School of Engineering and Management

Air Force Institute of Technology

Air University

Air Education and Training Command

In Partial Fulfillment of the Requirements for the

Degree of Master of Science in Electrical Engineering

Bryan S. Kim, B.S.E.E.

Second Lieutenant, USAF

March 2006

AFIT/GE/ENG/06-28

EVALUATING THE CORRELATION CHARACTERISTICS OF ARBITRARY AM AND FM RADIO SIGNALS FOR THE PURPOSE OF NAVIGATION

Bryan S. Kim, B.S.E.E.

Second Lieutenant, USAF

Approved:

/signed/	March 2006
Dr. Michael A. Temple (Chairman)	date

/signed/	March 2006
Dr. John F. Raquet (Member)	date

/signed/	March 2006
Maj. Todd B. Hale (Member)	date

AFIT/GE/ENG/06-28

Abstract

The Global Positioning System (GPS) provides position estimates on Earth at anytime, anywhere and in any weather. However, GPS requires an unobstructed path to satellite signals. As such, GPS performance generally degrades or becomes non-existent in environments such as large urban areas. This research investigates and analyzes the correlation characteristics of arbitrary AM and FM radio signals for the purpose of navigation. The primary objective of this research is to determine if there is any potential for using AM and FM radio signals in a TDOA-type navigation system. In support of this objective, two correlation receiver methods are considered with a goal of producing autocorrelation peaks between the received signals of the reference and target receivers. With successful results, hopefully future work can be done with these correlation methods and TDOA navigation techniques.

By using a reference signal with known characteristics (i.e., 31-Gold coded waveform), the integrity of the designed system model is validated by comparing simulated and theoretical results. Once the model performs as desired, the AM and FM radio signals are used as inputs. Simulations are conducted with different combinations of correlation methods ('fixed' or 'varying'), modulation types (AM or FM), and signal types (song or voice). Excluding reference signal validation results, there are eight different variations available for determining whether or not AM and FM radio signals have correlation characteristics useful for the purpose of navigation.

Out of the eight different variations considered, only two provided promising results for the purpose of navigation. Both the FM voice and FM song signals exhibit distinct autocorrelation peaks (i.e., 5.0 dB peak-to-sidelobe ratios) using the 'fixed' reference correlation method. However, results for both FM signal types revealed limited potential for navigation when using the 'varying' reference correlation method. All the AM signals considered yielded relatively limited potential for navigation using either correlation method.

iv

Acknowledgements

Thank you. I want to extend my thanks to everyone who has supported me and my efforts during this research. Many of you will go unnamed individually, but your support has been instrumental in the completion of this thesis and is far from unappreciated.

First, I would like to thank my thesis advisor, Dr. Temple. His insights, guidance and most importantly, his positive attitude throughout the whole process was vital for my success. I, as many of his other students, will always remember his many "Temple-ism" comments. *Press-on*, sir.

Second, I certainly cannot exclude my fellow students, especially my roommates: Dex, Matt, and Paul. Your friendships inside and outside the classroom has provided warm memories throughout our 18 month stay. I am privileged to have met each one of you and hope that our paths may cross in the future.

Finally, I want to express my love and gratitude for my family back home. They have always encouraged and believed in me. A part of everything I am is, and will always be, because of you. *Sa rang hae yo*.

Bryan S. Kim

Table of Contents

List of Figures

x

List of Tables

List of Symbols

List of Abbreviations

EVALUATING THE CORRELATION CHARACTERISTICS OF ARBITRARY AM AND FM RADIO SIGNALS FOR THE PURPOSE OF NAVIGATION

I. Introduction

This chapter provides the reason and goals for researching the correlation characteristics of arbitrary Amplitude Modulated (AM) and Frequency Modulated (FM) radio signals for the purpose of navigation. Section 1.1 explains the motivation and relevancy of this research. Section 1.2 discusses the two main goals set for this research model. Section 1.3 gives an overview of previous research done in related fields. An outline of the thesis is given in Section 1.4.

1.1   Motivation

The Global Positioning System (GPS) provides position estimates on the Earth at anytime, anywhere and in any weather. However, to provide robust positioning performance, GPS requires an unobstructed path to satellite signals. As such, GPS performance generally degrades or becomes non-existent in environments such as under dense vegetation, indoors, or in larger urban areas. So the use of non-GPS waveforms, commonly referred to as "signals of opportunity (SOP)" and including such signals as television broadcasts, cellular communications, AM radio, and FM radio, are being considered as alternatives for position estimation. The SOPs were specifically designed for purposes other than position estimation and are being studied to characterize navigation potential for non-GPS waveforms in urban areas [21]. This research investigates the correlation characteristics of arbitrary AM and FM radio signals for the purpose of navigation.

There is a great need for the military to develop non-GPS precision navigation technologies in order to be able to operate in environments where GPS is unavailable

1

[13]. Additional systems are needed to assist in the weaknesses of GPS or, in the worse-case unlikely scenario, backup and assume the responsibilities of GPS. The GPS is only a single system and a system failure could occur unexpectedly. There are other systems such as the Inertial Navigation System (INS) that can provide navigation capabilities, but these capabilities are only short-term and are not absolute position solutions [5]. So alternative systems need to be developed to backup or compliment the current GPS.

The aforementioned SOPs which are available as potential navigation signals include television broadcasts, cellular communications, AM radio, and FM radio. Each SOP has specific properties and characteristics that could be exploited for navigation however, AM and FM radio was selected for the following reasons.

The navigation potential of television broadcasting signals, or more specifically the National Television System Committee (NTSC) television broadcast signal, has been previously investigated in [5]. Follow-on work on the NTSC television broadcast could have been selected as the topic of this thesis, but there is interest in determining navigation potential for different waveforms.

Cellular communication waveforms, such as used for the Code Division Multiple Access (CDMA) IS-95 Digital Cellular Network, possess particular characteristics that make them potential candidates for navigation. The IS-95 Digital Cellular Network uses many signals and channels. One of the channels is called the pilot channel and this channel has a coded signal that allows the users to synchronize within the system. For every user or mobile on the system, the CDMA system assigns a specific digital code. These codes are so specific that multiple users can transmit simultaneously on the same frequency without interfering with each other [17]. The transmitted signal is a 32,767 bit pseudo-random "short" code that repeats 37.5 times per second [16]. Since this code is known along with other signal properties, correlation techniques can be used to estimate the time of signal reception. Position estimation can then be determined based on the time estimates of 4 or more independent signals. However,

the CDMA IS-95 network is an impractical alternative for GPS because it requires time-synchronization from GPS [5].

There are three reasons why the AM and FM radio signals were selected as the SOP of interest for this research. First, AM and FM radio signals are transmitted with more power and at a closer range than GPS signals. Approximately 50 watts of power are used to transmit signals from GPS satellites [14]. Typical AM and FM radio stations operate at transmit power levels up to 50 kilowatts [2]. Radio signals being transmitted at higher power correspond to stronger signals indoors and in urban areas. GPS signals typically cannot be received in these environments, but radio signals can be received. Second, the radio transmitters are stationary land-based locations whereas GPS has up to 32 orbiting satellites [14]. Stationary land-based locations not only allow for less complex navigation computations but more importantly, this eliminates some of the errors introduced by space-vehicle position and atmospheric effects [5]. Finally, radio signals are broadcasted at frequencies between 530 kHz to 1710 kHz for AM radio and between 87 MHz to 108MHz for FM radio. The carrier frequencies of GPS signals are 1227.6 MHz and 1575.42 MHz [14]. The number of different frequencies available for AM and FM radio signals improves system operability by giving the potential to avoid interference at a signal frequency [5].

1.2 Research Objectives

The main concept for this research is derived from the concepts developed in [5,7] for the NTSC television signal. The methodology and results between this thesis and the work done in [5,7] are quite different. The research documented in [5,7] dealt with the navigation potential of the NTSC broadcast signal, while this research investigates the Correlation Peak Identifiability (CPI) of arbitrary AM and FM radio signals. The promising navigation potential of the NTSC broadcast signal has increased curiosity regarding whether or not AM and/or FM radio signals have navigation potential using similar time-difference-of-arrival (TDOA) navigation methods. The main difference

3

between this research and [5, 7] is that [5, 7] already assumed the user knew which correlation peak was being tracked so that 'navigation potential' could be defined as the accuracy with which the user could estimate the time difference between a reference and target receiver. This research will determine how well the user will be able to distinguish and locate the correct correlation peak, thus the acronym CPI. In the real world, both the ability to locate the correct correlation peak and the ability to get accurate estimates of the time delay between the reference and target receivers are needed for navigation.

The TDOA navigation system is a range-based method of determining position by measuring the difference in arrival time of a signal between two receivers [31]. Two receivers, a reference receiver and a target receiver, are used to eliminate the need for any time synchronization in the signal of interest (SOI). The stationary location of the reference receiver is already known while the location of the mobile target receiver is at the point of interest. Since the location of the transmitter (i.e., signal source) is also known, once the SOI is received at both receivers and time-tagged, the time difference of how much more or less time the SOI took to get to the target receiver than the reference receiver can be determined. This time difference can then be converted to range using the speed of light. These range measurements tell how much closer or farther the target receiver was from the transmitter than the reference receiver was from the transmitter. So ultimately, the actual distance between the target receiver and transmitter can be calculated using TDOA [31]. Position estimation can then be determined based on the TDOA measurements from 4 or more independent signal sources. Three independent signal sources are needed for position while one independent signal source is needed to account for differential receiver clock error. In a real world application, the calculated range is actually a "pseudorange" meaning a measurement including range and clock error. Multi-lateration algorithms are then used on these pseudoranges to determine position estimation and clock errors [14]. These receiver clock errors while small can cause large error in position estimation and need to be accounted.

The CPI of arbitrary AM and FM radio signals for the purpose of navigation is investigated and analyzed based on the results of correlation functions. So the first objective of this research is to develop two separate correlation methods that will hopefully produce desired autocorrelation peaks using the received SOI of the reference and target receivers. Two approaches are developed to add diversity to the research. Ideally, the two correlation methods are developed so that any generic signal can be analyzed as the input signal and not just AM or FM radio signals. Models for the two correlation methods are developed, analyzed and verified by using a Gold coded BPSK waveform as the input signal. This waveform was chosen because it has known characteristics and correlation structure. With known characteristics, a comparison between the actual results and the theoretical results can be made to verify the performance of the models.

The primary objective of this research is to determine if there is any potential for using AM and FM radio signals in a TDOA-type navigation system by determining CPI. As a first step for assessing CPI, the results of two correlation models are analyzed when AM and FM radio signals are used as the input signal. The results from the correlation models will hopefully show some navigation potential so future work can be done with these correlation methods and TDOA navigation techniques.

1.3 Related Research

There are many related and similar topics on navigation systems already investigated and presented to the technical community. There is a study called radiodetermination which is "the determination of position, velocity and/or other characteristics of an object, or the obtaining of information relating to these parameters, by means of the propagation properties of radio waves [26]." There are two main types of radiodetermination. The first part of this section discusses the typical passive type of radiodetermination, radio location, while the second part of this section discusses the usually active type of radiodetermination, radionavigation. Different navigation systems within each radiodetermination category are also be presented.

1.3.1   Radiolocation - Passive Radiodetermination.   The passive type of radiodetermination is radiolocation which is the process of finding an object using radio waves [27]. The most well known system that uses radiolocation is the radar. A radar is considered a passive system because it finds the location of an object rather than actively finding one's own position. The location of the object can be determined from the angle at which the signal returns and/or the time it takes to return. These two techniques are most commonly seen in estimating the position of a mobile receiver. The angle-of-arrival (AOA) and time-of-arrival (TOA) measurement techniques are discussed below.

1.3.1.1   Angle of Arrival (AOA).   The AOA technique is the method of using angles between a receiver and transmitters to determine position. AOA requires, at least, the known location of two signal sources to determine the user's position in two dimensions. The user's position is located at the intersection point of the angle lines from each signal source. When the receiver locates each signal source, the individual signal angles are estimated by comparing either the signal amplitude or carrier-phase at an interferometer (i.e., multiple calibrated antennas) [1]. The signal amplitude comparison is less complicated than the carrier-phase method but it is also less accurate. The accuracy of a two antenna phase-comparison interferometer produces sub-degree angle estimations [22].

The AOA technique can be best seen with the classic example of how a ship determines its position using the known location of two landmarks (i.e., lighthouses or stationary buoys) [4]. With the use of a compass and map, the angle between the ship and two known landmarks can be drawn to show an intersection point. This intersection point is the position estimation for the two-dimensional case. This technique obviously has sources of error that degrade the position estimation accuracy. But the error can be reduced by using a third landmark. Figure 1.1 shows the AOA technique. Note that the center of the resulting triangle is the position estimation.
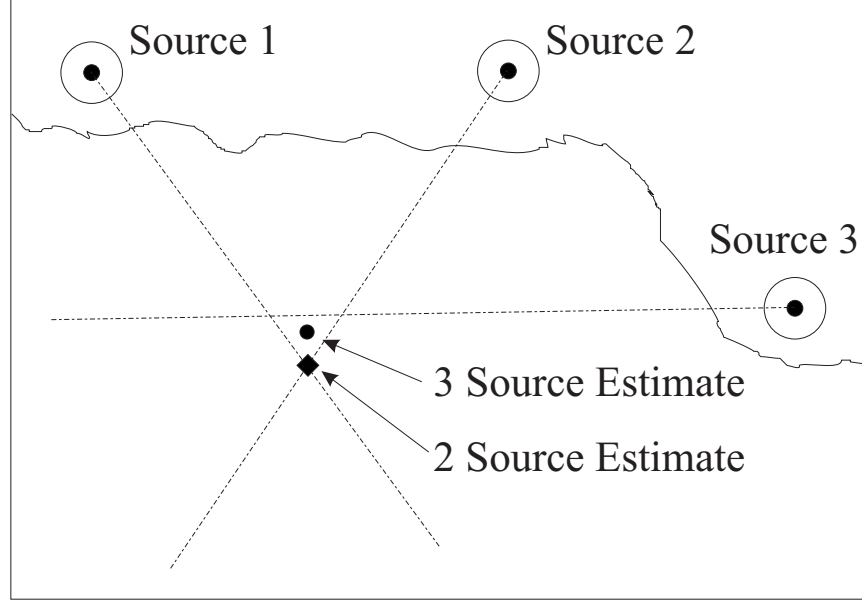
Figure 1.1:   AOA Position Estimate Technique using 2 or 3
Angle Measurements [5]

This estimation was determined by assuming all measurements and plots are equally accurate [5].

This passive navigation technique is a simple concept. AOA does not require extremely accurate time synchronization and it can easily incorporate any SOP in determining a location. The biggest downfall, however, is that AOA's accuracy is very range dependent. As the distance between the receiver and signal sources becomes greater, the errors in the direction measurement becomes greater producing larger position estimate errors [3].

1.3.1.2 Time of Arrival (TOA).   The TOA technique is the method of using propagation time of a signal between a transmitter and receiver to estimate range. This method does require precise time synchronization between all transmitters. Synchronizing the receiver clock is unnecessary because with all the transmitters synchronized, the receiver clock error is constant for all transmitters. This receiver clock error can be accounted for by doing one more additional measurement, allowing the error to be eliminated from the measurements [5]. So with the receiver knowing

the clock error and the times of transmission and arrival, the propagation time can be determined. And with the propagation times, position estimation can be calculated with trilateration. Trilateration is using measurements of TOA to estimate location using the intersection of hyperboloids [29].

      1.3.1.3 TOA Application - Trilateration.   The simplest of the basic principles of radio wave propagation is that waveforms travel at the known speed of light. Therefore, given this speed constant, the transit time of a signal from a transmitting station can be measured. Then using this transmit time, the distance between the transmitter and receiver can also be determined [10]. The receiver can compute its position unambiguously if given distances to three transmitters at known locations. The estimation of a position based on measurement of distances is referred to as trilateration. Another way to understand trilateration is to define it as the method of determining the relative position of objects using the geometry of circles [29]. This method of trilateration uses the known locations of two or more reference points, and the measured distance between the subject and each reference points. In general, at least three reference points are need to accurately and uniquely determine the relative location of a point on a two dimensional plane using trilateration. Figure 1.2 is an illustration of trilateration in two dimensions. P1, P2 and P3 are the known locations. With only one circle, the position estimation can be narrowed to anywhere on the P1 circle. The possible locations are then minimized to two points with the addition of the P2 circle. Points A and B are the intersection points to the P1 and P2 circles. Adding a third circle eliminates one of the two remaining points and identifies the true location B. This is an example of needing at least 3 reference points to accurately and uniquely determine the relative location of a point on a two dimensional plane using trilateration.

For generalization, the reason that three points are required lies in the geometry of circles. If the distance of a subject point from some fixed reference point, then that point could exist anywhere on a circle of that radius from the reference. If it is
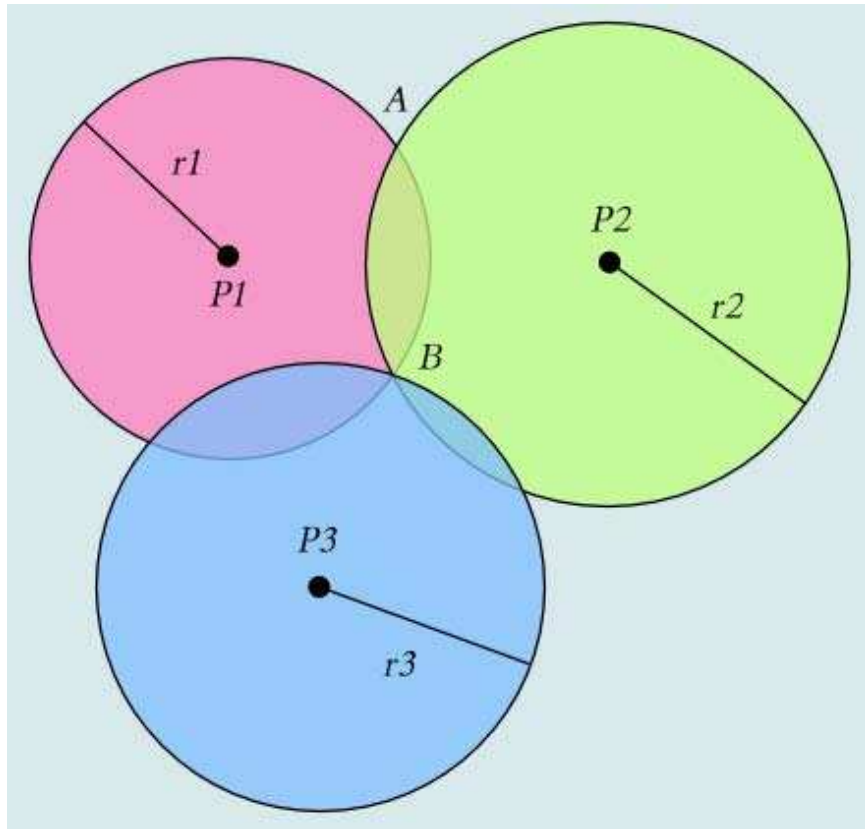
Figure 1.2:   Trilateration [29]

known that it is also a certain distance from a second reference point, then it also exists somewhere on a circle of that radius from the second reference point. These two circles almost always intersect at two points, and the subject could be at either point. In the case above, these points were A and B. The distance between the subject and a third reference point introduces a third circle into the diagram, and all three circles intersect at one point only. The position of the subject is relative to the three reference points [29]. This basic overview of trilateration assumes that the subject and the reference points all exist on one plane, implying that there are only two dimensions involved. For three dimensions, 4 reference points are needed and the subject point exists on the surface of 3-dimensional spheres instead of 2-dimensional circles. Two points almost always narrow it down to a circle, and three points to two points. Apart from those differences, the approach and technique are still the same. Note that in some real world applications that the minimum number of reference points may be required to disambiguate the subject's location. For example, in GPS if the subject is known to be on the surface of the Earth and the other intersection point is located in space, the point in space may be disregarded [14]. On the other hand, the stated number of reference points may not be enough if the geometry is singular [29].

1.3.2 Radionavigation - Active Radiodetermination. The active type of radiodetermination is the application of radio frequencies to determine a position on the Earth [28]. Radionavigation is very similar to radiolocation but rather than passively finding a distant object, radionavigation actively finds the user's location. The earliest radionavigation systems used celestial navigation methods. By using stars and planets, a person was able to determine his/her location on Earth. However this method only worked on clear nights. A different navigation method that would work in all weather and at all time of the day needed to be developed. So the first radionavigation system was developed, the radio direction finder (RDF). This system used an directional antenna to tune into a radio station. Since the directional antenna

was tuned into broadcasting antenna, the line of reception is also known. A current location could then be determined by taking two such measurements and plotting them on a map. Older systems used a hand-rotated loop antenna to find the angle of the signal. More modern systems use automated motorized directional solenoid to rapidly take measurements and then calculate the angle using computing software [28]. Not only were commercial AM radio stations used in this technology because of the long range and high power of AM signals, but strings of low-power radio beacons were also set up specifically for this system [28].

Other than GPS, there are other radionavigation systems that have been successfully implemented in the past, each of which is briefly described below.

1.3.2.1   Lorenz Navigation System.   The Lorenz or "Ultrakurzwellen-Landefunkfeuer" is a radionavigation system that was developed in the 1930s by the Germans as a night and bad weather landing system [25]. The basic concept of this system is to place a 'guiding beam' near the end of a runway to help navigate and land aircraft. The guiding beam has two signals broadcasted from highly directional antennas with each signal beam a few degrees wide. The signals are on the same frequency and transmitted at slightly different angles so that there is a small overlap in the middle of the guiding beam. Each signal was selected to emit a dash or a dot sound. When timed correctly, the dash and dot signals would link together producing one continuous sound in the overlapped section. Pilots were able to listen and determine where in the guiding beam they were in and respond accordingly [25]. The pilot's goal was to find the constant sound and remain on that course until the runway could be seen visually for safe landing.

1.3.2.2   VHF Omnidirectional Range (VOR).   The VHF omnidirectional range (VOR) navigation system is very similar to the Lorenz system but rather than use sound to navigate, VOR uses two signals that vary in phase to provide more accurate and reliable measurements. The first 'master' signal is transmitted continuously where in comparison, the second 'highly directional' signal is transmitted so
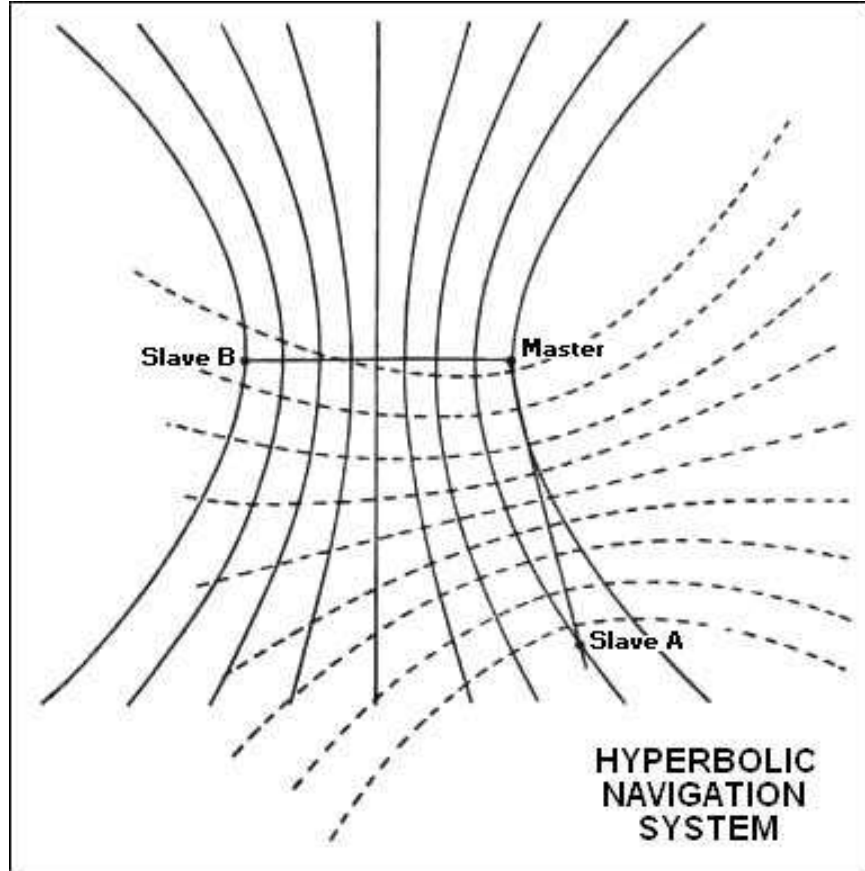
Figure 1.3:   GEE Navigation System [9]

that it varies in phase 3600 times a second faster. These signals are timed so that the phase varies as the secondary antenna rotates, such that when the antenna is 90 degrees from north, the signal is 90 degrees out of phase from the master [30]. By comparing the phase between the two signals, an angle can be determined and displayed for the pilot. Taking multiple such measurements, the aircraft location estimate can be made and used for safe landing [30].

1.3.2.3 GEE Navigation System.   The GEE or "AMES Type 7000" navigation system was developed by the British to determine aircraft or ship location by analyzing the delay times between two sets of signals [9]. Figure 1.3 illustrates the GEE navigation system. There are three transmitters including one 'master' and two 'slaves', 'A' and 'B'. By transmitting precisely timed signals, a user can analyze

the signal's time of arrival from each transmitter to determine relative location. For example, if signals from two transmitters arrive at the same time, the user must be equal distances from each signal source. This allows the user to draw a line on the map for all the positions that are equal distances from the transmitters. Taking similar measurements with other stations construct other lines, which hopefully lead to an intersection point [23]. This intersection point is the position estimation.

1.3.2.4   Long Range Navigation (LORAN).   The long range navigation (LORAN) system is a terrestrial navigation system that uses low-frequency radio transmitters to calculate time intervals between signal sources so that a position estimate can be determined [24]. LORAN was developed from the basic GEE principle and uses a similar master-slave transmitter network. However instead of using the same one-master/two-slaves arrangement as GEE, LORAN uses one master station and four to six slaves stations [24]. The master station broadcasts a series of short pulses which are received and re-broadcasted by multiple slave stations. The re-broadcasting by the four to six slave stations creates a chain-effect. Since the transmitters are synchronized, the time it takes for a radio signal to travel between transmitter stations and target receiver can be easily measured. With enough measurements, the hyperbolas will intersect providing a final position estimate [24].

1.4   Thesis Outline

Chapter I provided the motivation for researching the navigation potential of AM and FM radio signals as well as an overview of other related topics. *Chapter II* discusses the necessary background needed to understand the major concepts done in this research including trilateration, TDOA, filtering, autocorrelation, modulation, random binary waveforms, and the 31-Gold code. *Chapter III* describes the system model and parameters used to evaluate the CPI of arbitrary AM and FM radio signals for the purpose of navigation. *Chapter IV* presents simulated results and analysis conducted with the receiver model and two correlation methods developed. *Chapter V*

gives the overall system results and conclusions, followed by recommendations for further research in using AM and/or FM radio signals in a TDOA algorithm.

II. Background

This chapter provides the necessary background for the major topics in this thesis. Section 2.1 discusses the basic concepts of digital modulation. Section 2.2 provides the definition and relevant properties of autocorrelation. Section 2.3 explains the concepts needed to construct the 31-Gold random binary waveform, as used for a reference signal during code verification and validation. Section 2.4 provides the overall concept of TDOA.

2.1 Digital Data Modulation

Digital data modulation is a method of converting analog information, such as song or voice, to binary code for transmission. For baseband modulation, these waveforms are put onto a carrier wave to enhance transmission efficiency. Without the carrier modulation, signal transmission would require larger sized antennas. The antenna's physical size usually depends on the wavelength λ (λ = speed-of-light c / frequency f) and the application. For example, cellular telephone systems typically have antennas that are $\lambda/4$ in size. So without carrier modulation, it would take an antenna approximately 15 miles long to transmit a $f = 3000$ Hz baseband signal [18]. But with carrier-wave modulation at a higher frequency, i.e., $f = 900$ MHz carrier, the equivalent antenna diameter would be around 8 cm [18]. Therefore, carrier modulation is an essential step for all radio transmission systems.

Other than transmission efficiency using smaller antennas, carrier modulation provides additional benefits as well. Modulation is important in this research because it allows the user to place the SOI in a desired frequency band where designer requirements, such as filtering and amplification, can be easily met. This is the case where radio-frequency (RF) signals are converted to an intermediate frequency (IF) in the frontend of a receiver [18]. The following modulation properties are important for this research.

|X(f)|

A/2   A/2

-f_o   f_o

f
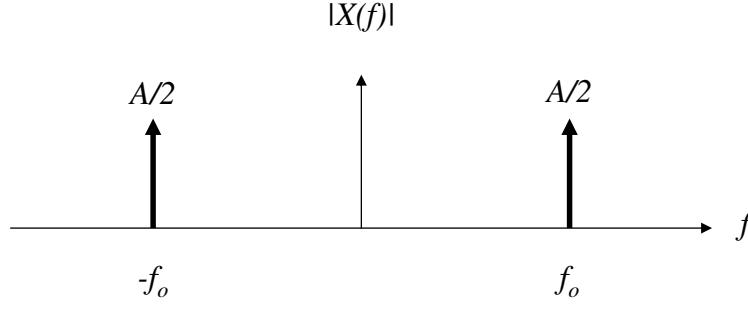
Figure 2.1:   Fourier Transform of Cosine [19]

Equation 2.1 shows the Fourier transform a cosine signal. The Fourier transform of the left-hand side results in a pair of delta functions located at $\pm f_o$ and having one-half the amplitude. Figure 2.1 shows the Fourier transform of (2.1).

$$A \cdot \cos(2\pi f_o t) \qquad \Longleftrightarrow \qquad \frac{A}{2} \cdot \{\delta(f - f_o) + \delta(f + f_o)\} \qquad (2.1)$$

Equation 2.2 shows the Fourier transform relationship for an arbitrary signal x(t) multiplied by the cosine function (the carrier modulation process). The Fourier transform of the left-hand side of (2.2) produces in the Fourier Transform of x(t) repeated at the carrier frequency of $\pm f_o$ and having one-half the amplitude.

$$x(t) \cdot \cos(2\pi f_o t) \qquad \Longleftrightarrow \qquad \frac{1}{2} \cdot \{X(f - f_o) + X(f + f_o)\} \qquad (2.2)$$

Equation 2.3 is the Fourier transform of an arbitrary signal x(t) multiplied by the sine function. The Fourier transform of the left-hand side results in the Fourier transform of x(t) repeated at $\pm f_o$ with $\frac{1}{2j}$ the amplitude. The Fourier transform for cosine and sine are identical except for the factor of $\frac{1}{j}$.

$$x(t) \cdot \sin(2\pi f_o t) \qquad \Longleftrightarrow \qquad \frac{1}{2j} \cdot \{X(f - f_o) - X(f + f_o)\} \qquad (2.3)$$

16

Table 2.1: Autocorrelation Properties for a Real-Valued Signal [18]

Property	Definition
$R_x(\tau) = R_x(-\tau)$	symmetrical in τ about zero
$|R_x(\tau)| \leq R_x(0)$ for all τ	maximum value occurs at the origin
$R_x(0) = \int_{-\infty}^{\infty} x(t)^2 dt$	value at the origin is equal to the energy of the signal

These fundamental modulation properties are important and are used for understanding the receiver model described in Chapter III. The frontend model within the receiver model, filters the incoming signal using bandpass filters centered around the carrier frequency f_o. To understand the frontend processing, one needs to understand what the modulation process does to the transmitted signal.

2.2 Autocorrelation

The autocorrelation function refers to the matching of a signal with a delayed version of itself [18]. Equation 2.4 is the autocorrelation function of a real-valued energy signal $x(t)$.

$$R_x(\tau) = \int_{-\infty}^{\infty} x(t)x(t+\tau)dt \qquad for -\infty < \tau < \infty \qquad (2.4)$$

Autocorrelation $R_x(\tau)$ can be used as an analytic tool to provide a measure of how closely a signal matches a copy of itself, as the copy is shifted τ units in time [18]. The variable τ is used as an iterating or scanning parameter. As listed in Table 2.1, there are autocorrelation properties that are useful for this research. The second property shows that the maximum autocorrelation value occurs at the origin ($\tau = 0$). This property is used in the correlation methods to track the signal.

2.3 Gold Coded, Random Binary Waveform

A 31-length Gold coded (31-Gold) random binary waveform (RBW) is used as the baseband reference signal for code verification and validation. The unique correlation properties of Gold coded waveforms permits testing of the accuracy and

| 1 | -1 | -1 | 1 | 1 | -1 | -1 | -1 | 1 | 1 | 1 | -1 | -1 | 1 | -1 | 1 | -1 | 1 | -1 | 1 | -1 | -1 | -1 | -1 | -1 | -1 | 1 | -1 | -1 | -1 | -1 | 1 | 1 |
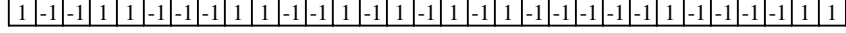
Figure 2.2:   31-Gold Code Sequence [20]

functionality of the designed system model described in Chapter III. There are three different concepts used to construct the 31-Gold coded RBW. The three concepts include the actual 31-Gold code sequence, the random binary waveform (RBW), and the binary phase shift keying (BPSK) modulation technique. The important details for each concept are given in the following subsections.

2.3.1 Gold Code Family of Sequences.   A Gold code family is a set of binary sequences which are commonly used in telecommunication. The Gold code used in this research is the 31-Gold code. The 31-Gold code sequence is shown in Figure 2.2. Note that $\pm 1's$ are used here to represent binary 0's and 1's, respectively. This particular 31-Gold code sequence is used to encode a RBW because it was a familiar sequence within telecommunications. A known sequence was needed for the verification/validation reference signal. Technically, this known sequence makes the RBW a pseudo-random binary waveform (PRBW), but is referred to as a RBW rather than a PRBW in this text.

2.3.2 Random Binary Waveform.   The random binary waveform (RBW) is a random process denoted as $X(t, A_k, D)$. The equation for the RBW is shown in Equation 2.5 [19].

$$X(t, A_k, D) = \sum_{k=-\infty}^{\infty} A_k p(t - kT - D) \tag{2.5}$$

where

$$p(t) = Rect\left(\frac{t}{T}\right) = \{ {1, \atop 0,} \quad {-T/2 < t < T/2 \atop otherwise} \tag{2.6}$$

18

Equation 2.5 is a function of two variables, including the discrete amplitude A_k of the kth symbol and the continuous delay D which is relative to the time origin. The t is a continuous time parameter and T is the symbol duration. The discrete amplitude A_k can be either -A or +A. The probability that A_k equals either $\pm A$ is equally likely at $\frac{1}{2}$.

Equation 2.7 is the autocorrelation of (2.5) and is denoted as $R_X(\tau)$ [19]. Note that the autocorrelation function is only a function of the time difference τ. This autocorrelation function makes intuitive sense because the correlation of two rectangles produces a triangle.

$$R_X(\tau) = A^2 Tri\left(\frac{t}{T}\right) = \begin{cases} A^2[1-\frac{|\tau|}{T}], & |\tau| \leq T \\ 0, & otherwise \end{cases} \tag{2.7}$$

Equation 2.8 is the Fourier transform of (2.7) and represents its PSD, denoted as $G_X(f)$ [19]. The Fourier transform property used to convert (2.7) to (2.8) is given in (2.9) [18].

$$G_X(f) = F\{R_X(\tau)\} = A^2 T sinc^2(fT) \tag{2.8}$$

$$Tri\left(\frac{t}{T}\right) \qquad \Longleftrightarrow \qquad T sinc^2(fT) \tag{2.9}$$

In summary, the RBW is a random process. The pulses are rectangular shaped with duration T. The pulses have random amplitude A_k values which are statistically independent and have equal probability of occurrence. The waveform has a random delay D which is uniformly distributed (i.e., U[t_o, t_o + T]).

2.3.3 Binary Phase Shift Keying.   Binary phase shift keying (BPSK) is perhaps the simplest case of phase shift keying (PSK). PSK was originally developed for deep-space programming but it is now widely used both within the military and commercial communication systems [18]. PSK is a method of digital communications

19

where the phase of a transmitted signal is varied to convey information. The general analytic expression for PSK is shown in (2.10)

$$s_i(t) = \sqrt{\frac{2E}{T}} \cos(2\pi f_o t + 2\pi \imath/M) \tag{2.10}$$

where $i = 1, 2, ..., M$, f_o is the carrier frequency, E is symbol energy, T is symbol time duration and $0 \leq t \leq T$. The phase term $\phi_i(t)$ is shown below

$$\phi_i(t) = \frac{2\pi \imath}{M} \tag{2.11}$$

where $i = 1, 2, ..., M$. This term has M discrete values.

For BPSK $M = 2$ and thus the modulating data shifts the phase of the waveform $s_i(t)$ to opposite values of $0°$ or $180°$ (zero or π). Substituting M $= 2$ into (2.11) simplifies the equation to positive multiples of π. So when phase terms in BPSK flips signs, the digital signal also flips signs. BPSK is sometimes called bi-phase modulation because there are only two possible phases [18].

2.3.4 31-Gold Code Signal Construction.   The concepts and information needed to construct the 31-Gold coded reference signal used for this research have now been presented. The following describes how all the concepts are put together to construct the reference signal used to verify the system model. Figure 2.3 shows the major parts within the transmitter. The RBW data information or bit stream $d(t)$ is input to the BPSK modulator at the data rate R_b. The BPSK modulator output $m(t)$ is then mixed with the RBW coded information waveform $c(t)$. The equation for $m(t)$ is shown in (2.12).

$$m(t) = d(t) \cos(2\pi f_o t) \tag{2.12}$$

The final transmitted signal is given by
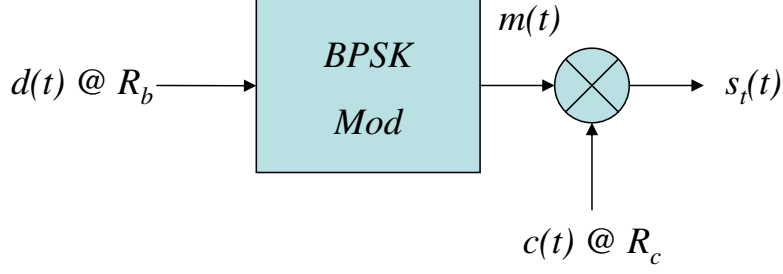
Figure 2.3:   BPSK Transmitter Model [19]

$$s_t(t) = \sqrt{2P_t}c(t)d(t)\cos(2\pi f_o t) \tag{2.13}$$

where P_t is the transmitter power, $c(t)$ is the 31-Gold coded RBW at the chip rate R_c, and $d(t)$ is the data modulation waveform at a bit rate R_D. For this research, the RBW data stream $d(t)$ is set to a constant value of 1 to simplify system model analysis. This is discussed again in Chapter III.

The PSD of the transmitted 31-Gold coded BPSK signal is given by

$$S_t(f) = \frac{P_t T_c}{2}\left\{sinc^2[(f + f_o)] + sinc^2[(f - f_o)]\right\} \tag{2.14}$$

where P_t is the transmitter power, T_c is the chip duration, and f_o is the carrier frequency. Note that the formula in (2.14) uses the concepts of 31-Gold code sequence, RBW, and BPSK modulation to construct this signal. Figure 2.4 shows the continuous PSD of the transmitted waveform. Note that the PSD is centered at positive f_o and has a null-null bandwidth of $2R_c$.

2.4   TDOA Positioning

The time difference of arrival (TDOA) algorithm is an extension of multilateration, or using distances from known locations to estimate position. The TDOA algorithm developed in the next section is a derivation of the LORAN system but
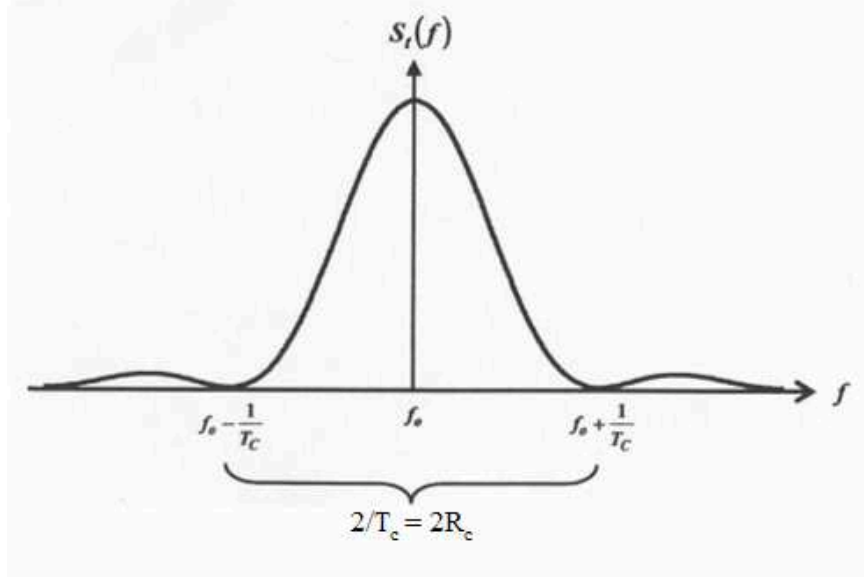
Figure 2.4:   Transmitted Waveform PSD (Continuous) [19]

differs in that it uses two receivers with one transmitter to estimate the range be-
tween one of the receivers and the transmitter [5]. This range provides a circle in two
dimensions of possible points for the target receiver around the transmitter. There
are two cases of the TDOA concept, TDOA with synchronized receivers and TDOA
with unsynchronized receivers. To better understand the overall picture, this section
concentrates on the less complicated TDOA concept using synchronized receivers.

The two receiver TDOA system requires that the transmitters and one of the
two receivers be static at a known location. The static receiver will be the reference
receiver and it must also have a real-time data link to the second mobile receiver at
the location of interest (target). Given this setup, the time the transmitted signal is
received is recorded at both the mobile and reference receivers. The reference receiver
sends this time of arrival to the target receiver which calculates the time difference
between the signals. This is converted to distance by multiplying by the speed of
light constant. The TDOA measurement is the only measurement needed to estimate
the range between the transmitter and target receiver, as the distance between the
transmitter and reference receiver is known. Since the two receivers are synchronized,
the clock errors will cancel out in the TDOA algorithm.

22
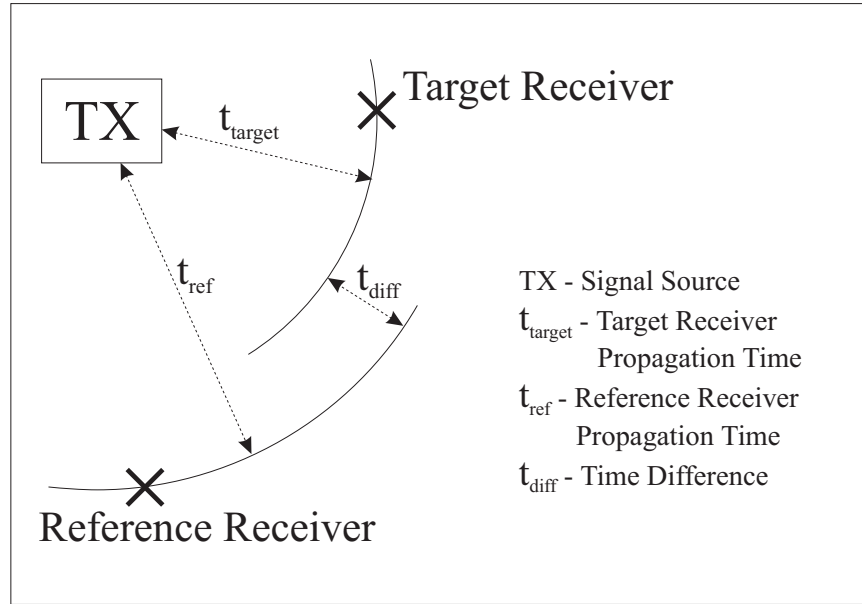
Figure 2.5:   Illustration of TDOA Range Estimates [5]
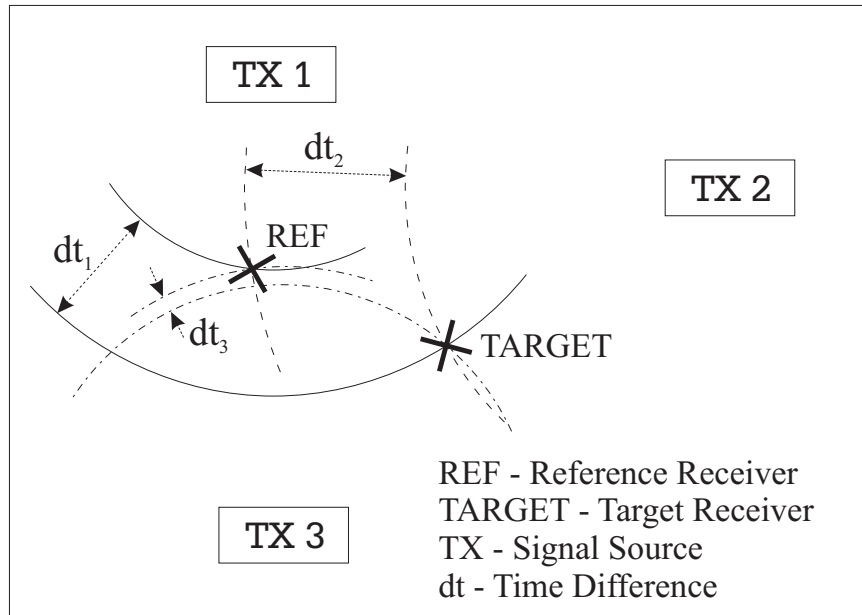
Figure 2.6:   Illustration of TDOA System with Three Signal Sources [5]

Figure 2.5 illustrates how the TDOA algorithm produces the range estimate for a single transmitter using the propagation time from both the mobile target and reference receivers. The time difference between the two receivers is the desired output instead of the actual time of each receiver when the signal was received [5]. Notice this figure is in the units of time and does not convert the times to distance. This conversion is just a scale factor of the speed of light and can be done later when needed. One can see that if the propagation time from the signal source to reference receiver is known, the difference in propagation times can be used to calculate the propagation times from the signal source to the target receiver. Then, if at least three signal sources are available, multi-lateration techniques can be used to estimate the target's receiver's position, as shown in Figure 2.6.

A general assumption for the system illustrated in Figure 2.6 is that all signals are measured at the same time or with a known time offset. Otherwise, the range estimates from each transmitter could be for different positions. However, if the target receiver is stationary this assumption is no longer required for the synchronized receiver case. First, to understand the effects of removing the synchronized receiver assumption, the local time for each receiver is defined in terms of some universal true time [5]:

$$\hat{t}_{ref} = t_{ref} + \epsilon_{ref} \tag{2.15}$$

$$\hat{t}_{tar} = t_{tar} + \epsilon_{tar} \tag{2.16}$$

where $\hat{t}_{ref}$ is the time according to the reference receiver clock, $\hat{t}_{tar}$ is the time according to the target receiver clock, t_{ref} and t_{ref} are the actual receiver times at the respective receivers, and then ϵ_{ref} and ϵ_{tar} are the respective clock errors in each receiver [5].

The TDOA measurement, incorporating these errors, then becomes:

$$TDOA = \hat{t}_{tar} - \hat{t}_{ref} \qquad (2.17)$$

$$= (t_{tar} + \epsilon_{tar}) - (t_{ref} + \epsilon_{ref})$$

$$= (t_{tar} - t_{ref}) + (\epsilon_{tar} - \epsilon_{ref})$$

$$= \frac{range_{ref} - range_{ref}}{c} + \delta t$$

where $\hat{t}_{tar}$ and $\hat{t}_{ref}$ are the TOAs according to the respective receiver clock, t_{tar} and t_{ref} are the true TOAs, $range_{tar}$ and $range_{ref}$ are the actual ranges between the transmitter and receivers, δt is the difference in clock errors and c is the speed of light.

Thus, the individual clock errors for each receiver have created an error in the TDOA measurement. More specifically, the TDOA measurement error is the difference between the receiver clock errors. If both errors were the same, the measurement error would be zero. This difference in local clock error is known as the clock bias and must also be estimated by the TDOA algorithm. The clock bias adds another unknown causing the required number of range estimates to increase to four for a three-dimensional position estimate.

Another subtle constraint added by the clock bias is all measurements must be taken simultaneously. The clock error for each receiver could change over time, and the TDOA algorithm only estimates a single value for all measurements. Fortunately, the drift rate statistics of many types of clock are known [5]. If the potential increase in error caused by this drift over the period in which samples are taken is acceptable, then the individual measurements can be taken sequentially.

Equation 2.17 defined the TDOA measurement in terms of actual values when the errors were known. The parameters as known to a physical system can be defined by rearranging that equation.

25

$$TDOA = \frac{range_{tar} - range_{ref}}{c} + \delta t$$

$$cTDOA = range_{tar} - range_{ref} + c\delta t$$

$$cTDOA + range_{ref} = range_{tar} + c\delta t \tag{2.18}$$

where $cTDOA + range_{ref}$ is the "pseudorange-like" measurement, $range_{tar}$ is the actual range, and $c\delta t$ is the clock bias in units of meters.

Note that this is essentially equivalent in form to a GPS pseudorange measurement, which is the combination of true range and clock error [22].

2.5   Summary

This chapter provided the necessary background for the major topics in this thesis. The basic digital communication concepts needed to construct the 31-Gold coded BPSK reference signal were presented and discussed. The definition and relevant properties of autocorrelation were also discussed along with the concepts of TDOA. All the topics discussed in this chapter help with understanding the research methodology as presented in Chapter III.

III. Methodology

This chapter describes the system model and parameters used to evaluate the correlation characteristics of arbitrary AM and FM radio signals for the purpose of navigation. Section 3.1 explains the basic model setup and the frontend design of the receiver model. Section 3.2 discusses the three signal types used in the research model. Section 3.3 develops two different correlation approaches used for determining if the signal of interest (SOI) has any correlation characteristics useful for the purpose of navigation. Section 3.4 clarifies how the term 'navigation potential of a signal' is defined and determined in this research. A summary is given at the end of this chapter.

3.1   Model Development

Before the Correlation Peak Identifiability (CPI) of a particular SOI can be determined, an accurate model must be developed to analyze and evaluates the acquired signals. This section discusses the development of the model used for this research.

3.1.1   Basic Model.   The basic transmitter and receiver model used in this research is shown in Figure 3.1. A signal $s_t(t)$ is transmitted from a known location through a channel to a target receiver. The transmitted signal $s_t(t)$ ideally can be any type of signal. The signal received at the receiver's antenna $s_r(t)$ is the acquired
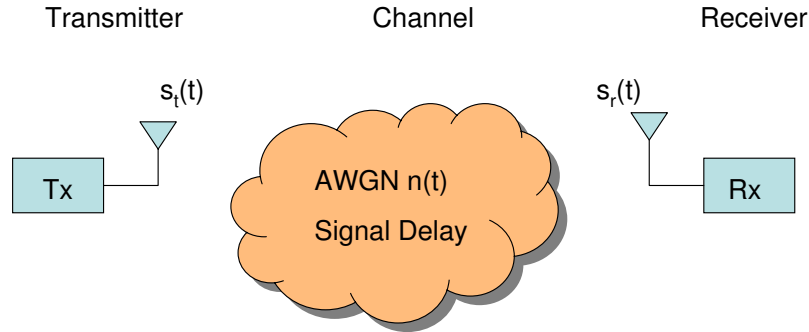
Figure 3.1:   Basic Transmit-Receive Model
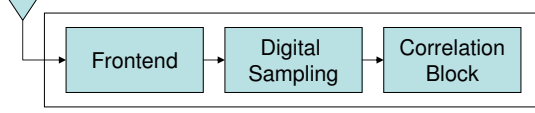
Figure 3.2:   Major Receiver Components

signal used for potential navigation. A general expression for received signal $s_r(t)$ in terms of transmitted signal $s_t(t)$ is given by

$$s_r(t) = s_t(t - C_d) + n(t) \tag{3.1}$$

where the signal propagation delay C_d and additive-white-gaussian-noise (AWGN) $n(t)$ factors are included in the received response of (3.1) to make it more realistic.

   3.1.2   Receiver Frontend Model.   The three major components of the receiver model are shown in Figure 3.2. The first receiver model component is the frontend. The purpose to the receiver frontend is to process and convert the high frequency input signal into a signal that is more suitable for signal processing and analysis. The receiver frontend model is shown in Figure 3.3. The input signal $s_t(t)$ is received at the antenna. The signal is then filtered at a specific radio frequency f_{RF} to extract the relevant signal energy. The output to H_{RF} is the radio frequency (RF) filtered signal denoted as s_{RF}. Although a majority of the noise in s_{RF} is filtered out, the signal still

28

exists at the carrier frequency of $s_r(t)$. The carrier frequency can be removed using down conversion. A local oscillator (LO) signal is generated at the carrier frequency to mix with s_{RF} and down-convert the signal to baseband. The LO signal (s_{LO}) can be expressed as

$$s_{LO} = A \cdot \cos(2\pi f_c t) \tag{3.2}$$

where A is an arbitrary amplitude, f_c is the carrier frequency and t is the time.

Mixing s_{RF} and s_{LO} produces the In-phase (I) signal response $x_I(t)$ given by.

$$x_I(t) = s_{RF} \cdot A \cos(2\pi f_c t) \tag{3.3}$$

By phase shifting s_{LO} by 90 degrees, the Quadrature-phase (Q) signal response $x_Q(t)$ is generated. Accounting for these changes in Equation 3.2 and Equation 3.3 yields the following:

$$s_{LO} = A \cdot \sin(2\pi f_c t) \tag{3.4}$$

$$x_Q(t) = s_{RF} \cdot A \sin(2\pi f_c t) \tag{3.5}$$

Once the In-phase and Quadrature (I&Q) mixed signals are produced, the signals are filtered through a baseband (BB) filter (H_{BB}) to complete the down-conversion process. At this point, the received RF signal exists at a baseband frequency. The output signals from the H_{BB} filters are the I&Q experimental data. The I&Q experimental data is denoted as $z_I(t)$ and $z_Q(t)$, respectively. This receiver frontend process filters, mixes and filters the input signal down to the baseband frequency where it is digitally sampled. The frontend process is called 'conditioning the received signal'. Note that the digital sampling process is the second of three major receiver model components shown in Figure 3.2.
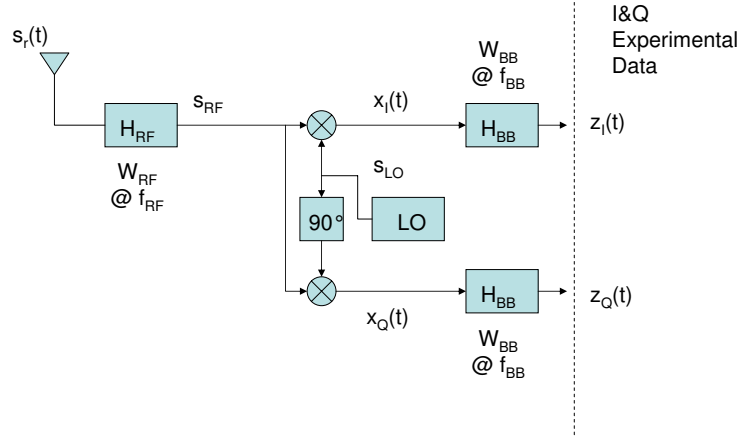
Figure 3.3:   Receiver Frontend Model

The filters in this model were designed based on the specifications of each SOI. One type of filter was used in this research, the finite impulse response (FIR) 2nd-Order Butterworth filter. This selection was made based on ease of implementation in simulation. There are other advanced filters which exist that have better characteristics such as sharper transitions between passband and stopband, more attenuation and less ripple in the stopband, and less phase delay [5]. However, using such an advanced filter was not necessary for the scope of this research. High fidelity filter characteristics, such as the precise bandstopping capability at the edges of the pulses, were not critical to evaluating overall system performance. The filters were designed to induce general effects of bandlimiting the signal while capturing a majority of the signal energy within the filter bandwidth. Problems that usually arise from using FIR filters such as Gibbs phenomenon or ringing at discontinuities did not have an extreme affect on the process [5]. If the research required, the phenomenon can be reduced by windowing, but it can never be completely eliminated in FIR filters. There are other filters that avoid this phenomenon, such as infinite impulse response (IIR) filters, but with the tradeoff of increased signal processing [15].

3.2 Signal Types

There are three different signal types used in this research. The three SOIs considered include a 31-Gold coded random binary waveform (RBW), the AM radio waveform and the FM radio waveform. The structure and details for each of the waveforms are given in the following subsections.

3.2.1 31-Gold Coded Random Binary Waveform.   The first step in determining the accuracy and functionality of a designed system model is to test the process with a known input and analyze the results of the output. The known input for this research is a 31-Gold Coded RBW. The statistics for the spreading waveform $C(t)$ used to construct the RBW are given in Table 3.1. Note that one second of the spreading waveform contains one symbol, there are 31 chips/symbol, with 50 samples/chip, and thus a total of 1550 data samples/symbol. The number of symbols in the waveform used for this simulation was set at 3 symbols. This number is somewhat arbitrary and was set based on simulation capability.

The equation for a 31-Gold coded RBW is shown in Equation 3.6 [8] which not only contains the spreading code but also the information data stream $d(t)$ and the noise

$$s_{RBW} = C(t)d(t)\cos(2\pi f_c t) + n(t) \tag{3.6}$$

where $C(t)$ is the spreading waveform, $d(t)$ is the information data stream, f_c is the carrier frequency, t is the time, and $n(t)$ is the AWGN.

The 31-Gold coded RBW is the initial signal used to test the integrity of the system model. For analysis purposes, the information data $d(t)$ was set equal to a constant value of 1. This simplification reduces Equation 3.6 to

$$s_{RBW} = C(t)\cos(2\pi f_c t) + n(t) \tag{3.7}$$

Table 3.1:   Statistics of 31-Gold Spreading Code

Statistics	Value
Number of Chips per Symbol	31
Symbol Duration	1.0 sec
Chip Duration	0.0323 secs
Samples per Chip	50
Carrier Frequency f_c	155 Hz
Time between Samples $\triangle t$	6.4516e-4 secs
Sample Frequency f_s	1550 Hz

A segment of the signals are shown in Figure 3.4. The top plot shows the $C(t)$-plus-noise signal and the bottom plot shows the carrier modulated $C(t)$-plus-noise signal. Note the corresponding sign changes between the RBW and the final received signal. This carrier modulated RBW is used as the initial verification signal because the structure of the waveform and its correlation characteristics are known, i.e., the received signal is a periodic waveform with a known spreading code modulated onto it. The known properties and structures of this input signal allows the user to predict the model results. If the actual results are consistent with the expected results, then the user can are confident that the system model is performing as designed (verification).

3.2.2   AM and FM Radio Waveforms.   The AM and FM radio signals used in this research were created by taking real baseband data (voice and song) and then modulating the data onto a carrier using software to simulate the real-world radio signals. The baseband data was stored in a *.wav data format. The normalized baseband song and voice signals are shown in Figure 3.5 and Figure 3.6, respectively. In these figures, the top plot is the full time duration of the signals, the middle plot is a zoomed-in version and the bottom plot is the power spectral density (PSD). Using Matlab®, the data for both the voice and song baseband signals were amplitude and frequency modulated as described in the following subsections.
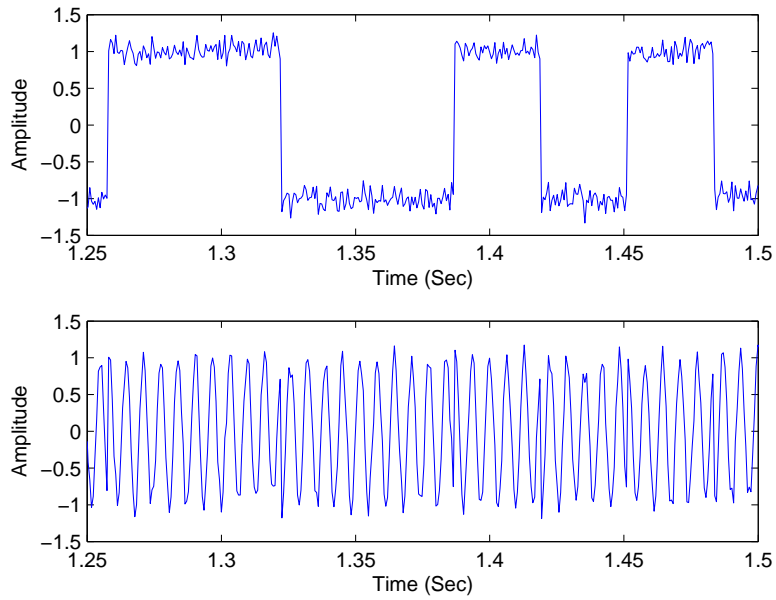
Figure 3.4:   31-Gold Coded Random Binary Waveform: Baseband (top) and Carrier Modulated (bottom)
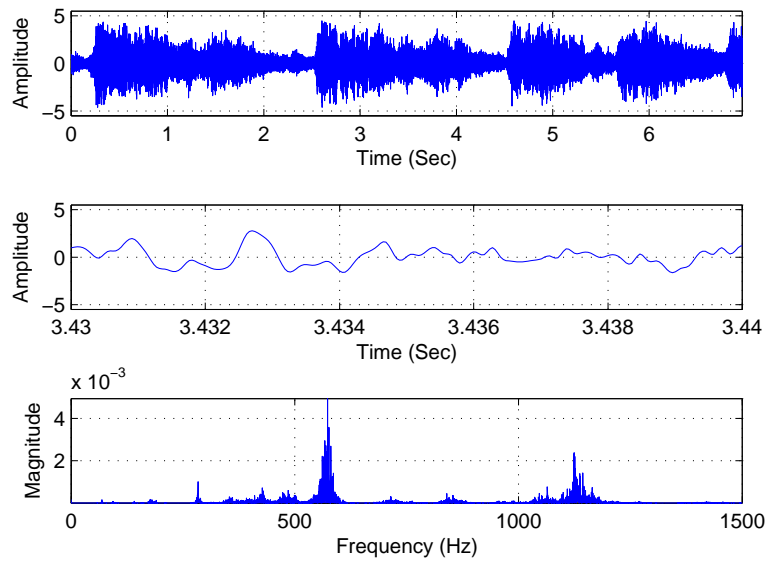
Figure 3.5:   Baseband Song Signal: Full Duration (top), Expanded View (middle), and Power Spectral Density (bottom)
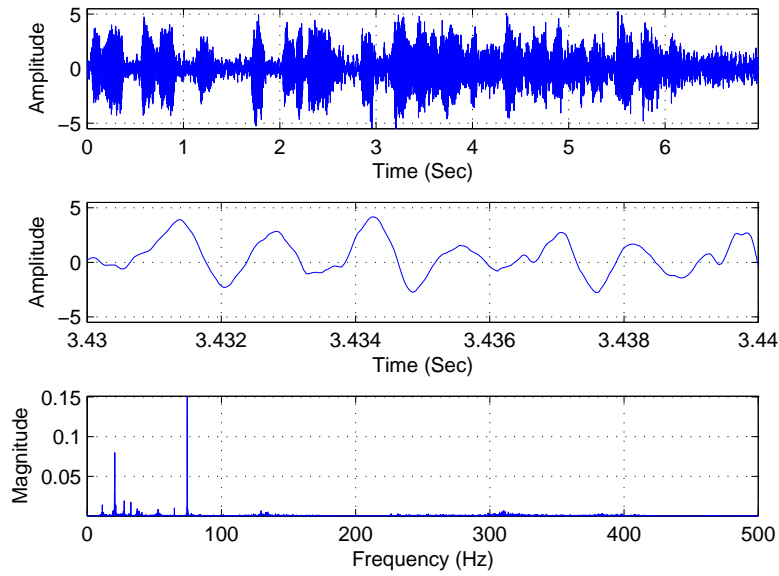
Figure 3.6: Baseband Voice Signal: Full Duration (top), Expanded View (middle), and Power Spectral Density (bottom)
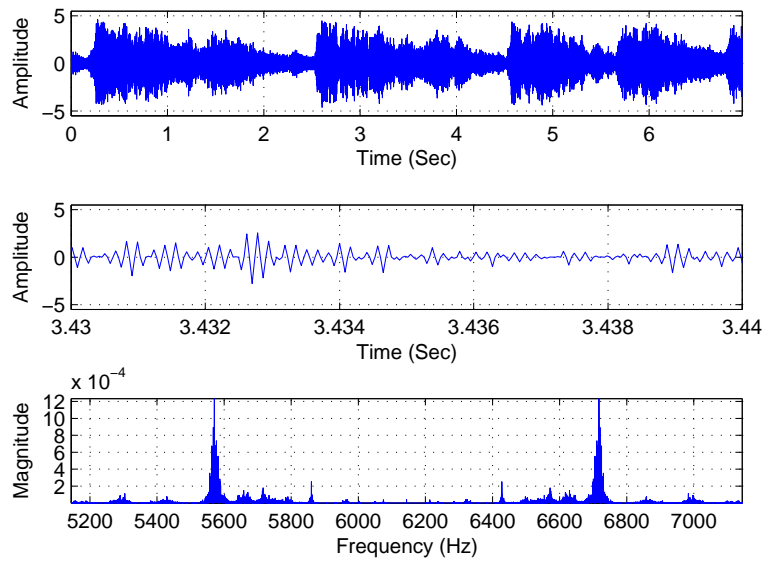
Figure 3.7: *AM Song* Signal: Full Duration (top), Expanded View (middle), and Power Spectral Density (bottom)

Figure 3.8:   *AM Voice* Signal: Full Duration (top), Expanded
View (middle), and Power Spectral Density (bottom)

3.2.2.1   AM Radio Waveform.   Amplitude modulation (AM) is the
technique of varying the amplitude, or strength, of a radio signal in accordance to the
voice or music being transmitted [11]. The interest in using the AM radio signal as
a SOI is based on the fact that AM radio technology is available world-wide and the
coverage of AM frequencies is broader than FM radio.

AM radio signals are electromagnetic waves with frequencies between 535 kHz
and 1605 kHz [12]. However the obtained baseband data was sampled at a frequency
of 24576 Hz. And the carrier frequency must be at most half the sampling frequency.
So for testing and simulation purposes, the normalized baseband data was modulated
at fourth of the sampling frequency, 6144 Hz.

Figure 3.7 and Figure 3.8 are the AM normalized baseband song and voice
data, respectively. The top plot shows the entire AM song signal while the middle
plot shows the zoomed-in version. The bottom plot shows the PSD.

35

Figure 3.9:   *FM Song* Signal: Full Duration (top), Expanded
View (middle), and Power Spectral Density (bottom)

3.2.2.2   FM Radio Waveform.   Frequency modulation (FM) is the
technique of varying the frequency of a radio signal in accordance to the voice or
music being transmitted [11]. The interest in using the FM radio signal as a SOI is
based on the fact that the overall trend of FM radio signals are better quality than
AM radio signals. FM radio signals have less susceptible to static which hopefully
corresponds with higher potential for navigation.

FM radio signals are electromagnetic waves with frequencies between 88 MHz
and 108 MHz [12]. However the obtained baseband data was sampled at a frequency
of 24576 Hz. And the carrier frequency must be at most half the sampling frequency.
So for testing and simulation purposes, the normalized baseband data was modulated
at fourth of the sampling frequency, 6144 Hz.

Figure 3.9 and Figure 3.10 are the FM normalized baseband song and voice
data, respectively. The top plot shows the entire AM song signal while the middle
plot shows the zoomed-in version. The bottom plot shows the PSD.

36
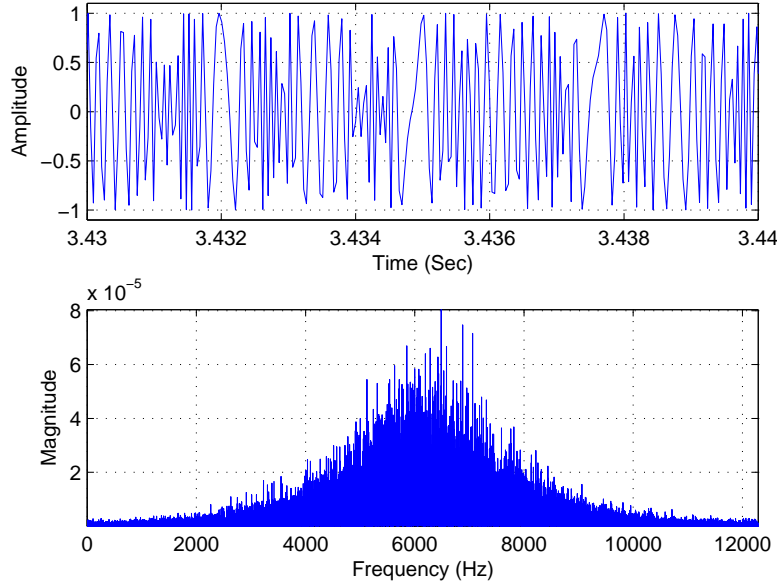
Figure 3.10:   *FM Voice* Signal: Full Duration (top), Expanded
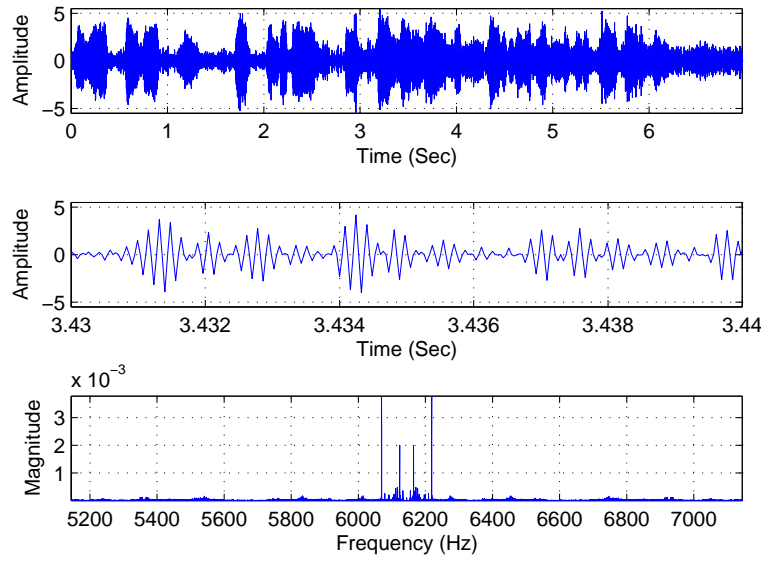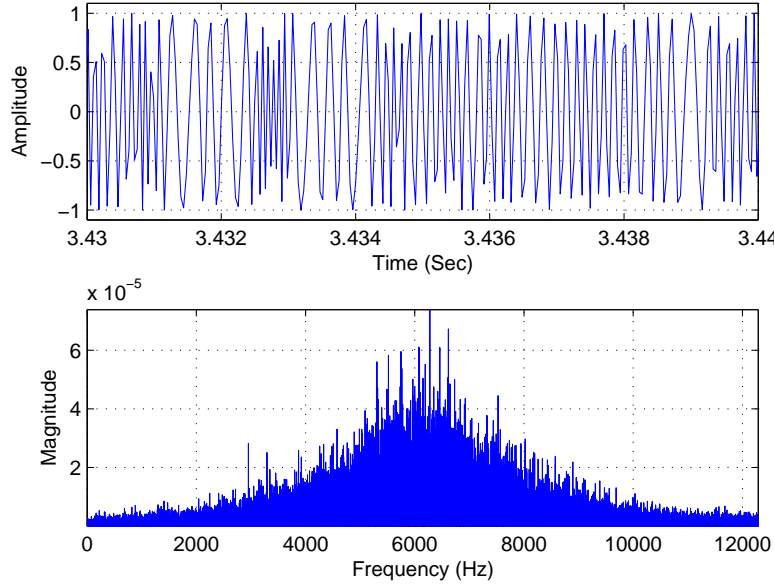View (middle), and Power Spectral Density (bottom)

3.3   Correlator Development

The third and final major component of the receiver shown in Figure 3.2 is the
correlation block. Once the receiver has conditioned the received signal by filtering the
noise and removing the carrier, the data can be stored and correlated with data from
another receiver. Navigation is done by determining the TDOA between two receivers'
data as discussed in Section 2.4. The two different correlation approaches shown in
this section are designed to account for multiple delay values which correspondingly
simulate multiple receivers at different locations.

3.3.1   Correlation A: "Varying" Reference Correlation.   The first correlation
approach is referred to as the "varying-reference" method. The varying reference
corresponds to changing correlation window when each correlation iteration is being
done. This correlation method is depicted in the diagram shown in Figure 3.11 where
N_w is the width of the correlation window and Δw is the number of samples shifted
between correlation calculations. In this case, the input signal $z(t)$ is multiplied by
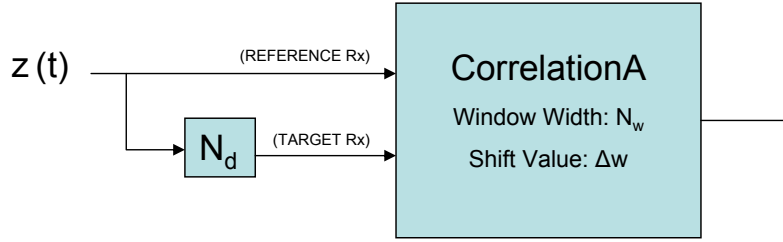
Figure 3.11:   Correlation A - "Varying" Reference Correlation

the delayed version of itself $z(t - T_D)$. The undelayed and delayed signals represent the received signals from the reference and target receivers, respectively. Once the two signals are multiplied, correlation between the delayed and undelayed signal can be determined. This method of correlation is intended to represent a real-time (analog) correlation process.

The best way to explain how the Correlation A process was designed is operate is via example as shown in Figure 3.12. The undelayed signal is shown by sample indexes. The delayed signal is delayed by 3 samples (N_d) and shown below the undelayed signal. The two signals are then multiplied sample-by-sample. After multiplication, the first correlation value at iteration $i = 1$ is calculated by summing up the samples within a correlation window. The correlation window size (N_w) is indicated by the shaded area which is $N_w = 5$ samples for this example. The next correlation value for iteration $i = 2$ is calculated after shifting the correlation window by Δw samples. The process of shifting the correlation window between iterations is why the terminology "varying" reference is applied to this correlation method. The shift value of the window (Δw) is set to 1 for this example. So for a total signal length of (N_i), the correlation window is shifted or "varied" by Δw between each correlation iteration until all N_i values have been correlated across. This model is designed to account for multiple delays (variable 'N_d' in Figure 3.11) which simulate multiple locations of the target receivers.

Example: Nd = 3, Nw = 5 and Δw = 1

varying reference Nw = 5

x_undelay

| 1 | 2 | 3 | 4 | 5 | 6 | 7 | 8 | 9 | 10 | 11 | 12 | ... |

⊗ i = 1

x_delay

| | | | 1 | 2 | 3 | 4 | 5 | 6 | 7 | 8 | 9 | ... |

shift Δw = 1

| 1 | 2 | 3 | 4 | 5 | 6 | 7 | 8 | 9 | 10 | 11 | 12 | ... |

⊗ i = 2

| | | | 1 | 2 | 3 | 4 | 5 | 6 | 7 | 8 | 9 | ... |

shift Δw = 1

| 1 | 2 | 3 | 4 | 5 | 6 | 7 | 8 | 9 | 10 | 11 | 12 | ... |

⊗ i = 3

| | | | 1 | 2 | 3 | 4 | 5 | 6 | 7 | 8 | 9 | ... |

time index   t1 t2 t3 t4 t5 t6 t7 t8 t9   ...   tNi

Figure 3.12:   Example Illustrating Three Iterations of "Varying" Reference Correlation

(REFERENCE Rx)

Store N_w

CorrelationB

Window Width: N_w

Shift Value: Δw

$z(t)$

N_d (TARGET Rx)
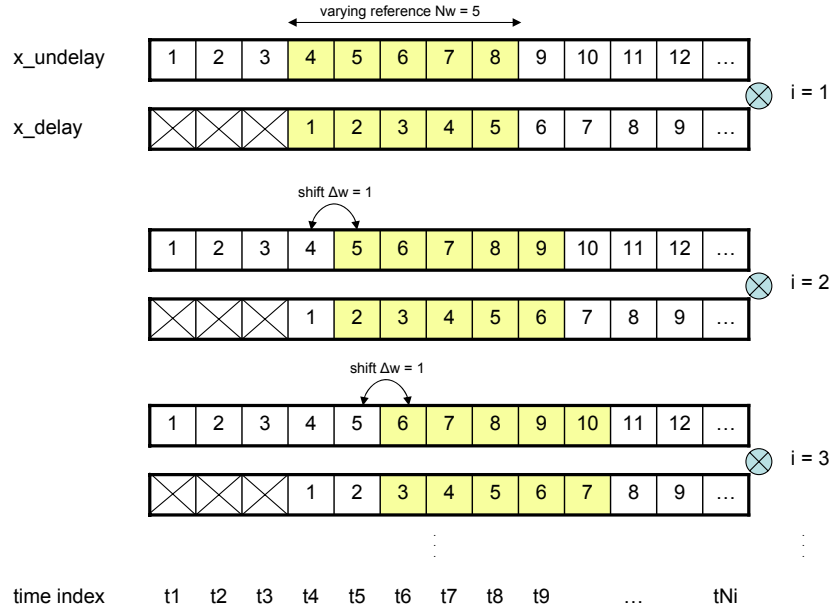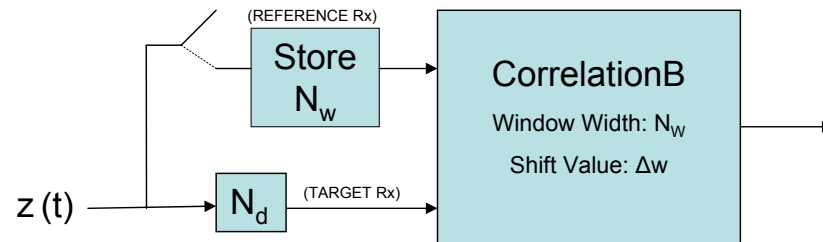
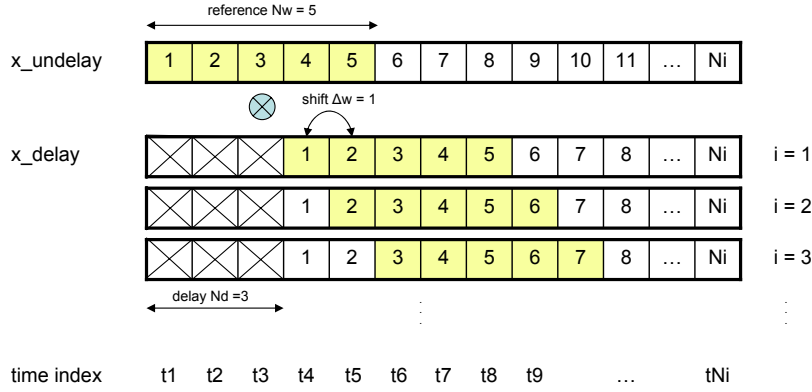Figure 3.13:   Correlation B - "Fixed" Reference Correlation

Figure 3.14:   Example Illustrating Three Iterations of "Fixed" Reference Correlation

3.3.2   Correlation B: "Fixed" Reference Correlation.   The second correlation approach is referred to as the "fixed-reference" method. The fixed reference corresponds to the fixed correlation reference window when each correlation iteration is being done. This correlation method is depicted in the diagram shown in Figure 3.13. In this case, an N_w segment of the undelayed signal is stored (fixed-reference window) and used as a reference correlation signal across the entire delayed signal. The undelayed signal represents the signal from the reference receiver. The delayed signal represents the signal from the target receivers. Once the fixed-reference window is stored, correlation between the fixed-reference and the delayed signal can be determined.

The best way to explain how the Correlation B process was designed to operate is via example. Three iterations of the fixed-reference correlation method is shown in Figure 3.14. The example shows the fixed-reference being set to the first 5 samples of the undelayed signal. For the first $i = 1$ iteration the correlation value is calculated by multiplying and summing up the samples within a correlation window. The correlation window size (N_w) is indicated by the shaded area which is $N_w = 5$ samples for this example. The next correlation value for the $i = 2$ iteration is calculated by taking the same fixed-reference window and shifting it to the right along the delayed signal

by Δw. The notion of keeping the same reference window and shifting along the delayed signal between iterations is why the "fixed" reference terminology is applied to this correlation method. The window shift value (Δw) is set to 1 for this example. So for a total length data signal of N_i samples, the fixed-correlation window is shifted by Δw between each correlation iteration until all N_i values have been correlated across. This model is designed to account for multiple delays (variable 'N_d' in Figure 3.13) which simulate multiple target receiver locations.

3.4 Definition of Navigation Potential

The main concept for this research is derived from the concepts developed in [5,7] however the methodology and results between this thesis and the work done in [5,7] are quite different. The main difference between this research and [5,7] is the definition of 'navigation potential'. The research in [5,7] already assumes the user knows which correlation peak is being tracked so that 'navigation potential' could be defined as the accuracy with which the user could estimate the time difference between a reference and target receiver. Navigation potential in this research is determined by how well the user will be able to distinguish and locate the correct correlation peak, or Correlation Peak Identifiability (CPI). In the real world, both the ability to locate the correct correlation peak and the ability to get accurate estimates of the time delay between the reference and target receivers are needed for navigation.

The navigation potential of the signals presented in Chapter IV will be based on one determining factor. The signal will be categorized as 'promising potential' if any arbitrary segment of the signal can be used to produce a distinguishable autocorrelation peak. Otherwise the signal will be categorized as 'limited potential'. Navigation potential in this research will interpreted as the ability to distinguishably locate the correct autocorrelation peak, CPI, regardless of the signal segment selected. Again, note this is not the same definition used in [5,7].

3.5 Summary

This chapter describes the overall transmit-receiver system model and parameters used to evaluate the CPI of the AM and FM radio signals for the purpose of navigation. The basic model setup and the receiver frontend design were discussed as well as the three signal types used in the research. Two different correlation approaches were introduced for determining if the signals of interest have any navigation potential. The term 'navigation potential' and CPI are also defined to help clarify the conclusions drawn from the Chapter IV.

IV. Simulation Results and Analysis

This chapter presents simulated results and analysis conducted with the receiver model and two correlation methods described in Section 3.1 and Section 3.3, respectively. Section 4.1 provides model verification by presenting and analyzing simulation results for the 31-Gold Coded RBW signal. Section 4.2 shows and discusses the results of the model when AM radio signals are used as the input waveform. Section 4.3 repeats the analysis but for FM radio signals as the input waveform. Each radio signal section conducts an analysis with both song and voice type waveforms and both correlation methods. The correlation results will help determine if navigation is possible for each case.

4.1 Model Verification

Before the CPI of a particular SOI can be determined for the purpose of navigation, an accurate model must be developed to analyze and evaluate the acquired signals. This section shows the model results when using the periodic 31-Gold coded RBW as the input signal. Due to the known characteristics of the signal, the actual results can be compared to the theoretical results to verify the model's process. The validation results are shown in this section and organized into three parts. The parts are represented as frontend results, correlation method results when varying delay and correlation method results when varying correlation window size. Correlation method results are shown in raw and normalized-dB scale forms.

4.1.1 Frontend Model Results and Analysis. The following results are presented to verify the frontend process. As designed, the frontend model performs well in conditioning the received signal into a noise-reduced baseband signal. The process is similar for all of the correlation-waveform type cases so only one set of step-by-step results and analysis are discussed. For the remainder of the frontend process results, only the signals before and after the conditioning process will be shown. The filter bandwidths used in the simulation for each signal are summarized in Table 4.1.
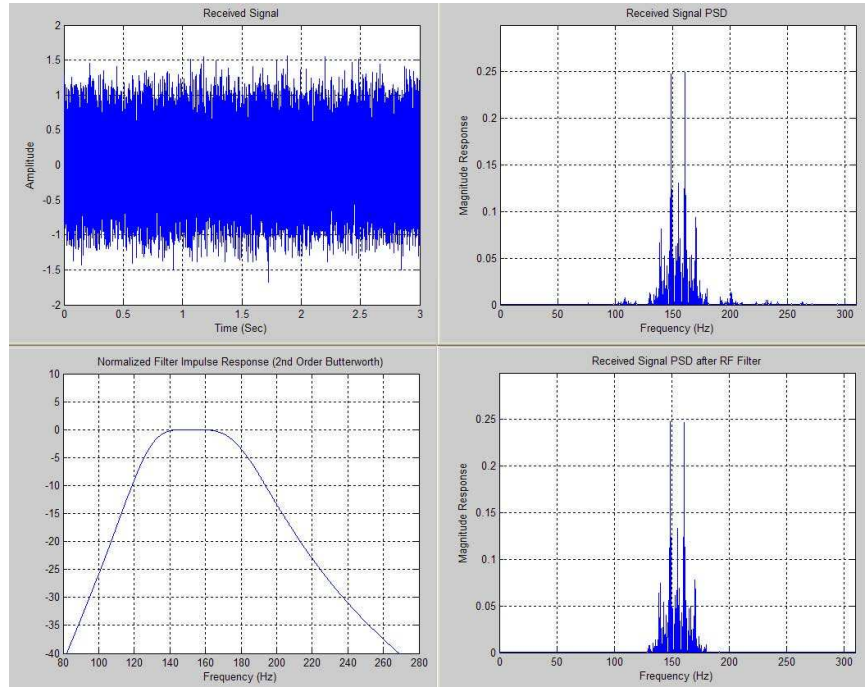
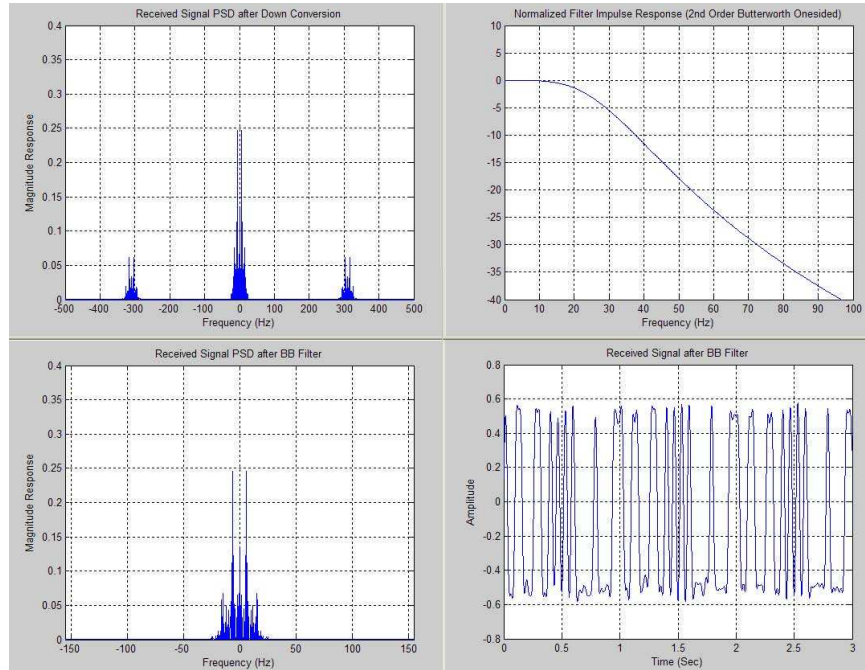Figure 4.1:   Frontend Process - RF Filter Results

Figure 4.2:   Frontend Process - Downconversion and BB Filter Results

Table 4.1:   Bandwidth for Frontend Process Filters

Signal Type	H_{RF}	H_{BB}
31-Gold coded RBW	101 Hz	99 Hz
AM Song	1057 Hz	1044 Hz
AM Voice	161 Hz	162 Hz
FM Song	2114 Hz	2088 Hz
FM Voice	322 Hz	324 Hz

Note that the center frequency used for the passband H_{RF} filters was 155 Hz for the 31-Gold coded RBW signal and 6144 Hz for the AM and FM radio signals.

The frontend process is validated by using the 31-Gold coded signal as the input waveform. Figure 4.1 shows the results for the RF filter portion of the frontend process. The top row of figures are the received signal and PSD of the received signal. The received signal appears noise-like but the PSD shows a majority of signal energy centered approximately around 155 Hz. This result makes sense since the carrier wave frequency was set to 155 Hz in the simulation. The bottom row of figures show the RF filter response and the PSD of the received signal after the RF filter. The RF filter used, as mentioned in Section 3.1, is a 2nd-order Butterworth filter. Note the PSD of the received signal before and after RF filtering. The after-picture reveals the before-PSD with a majority of the original energy but without some of the noise spikes. This result indicates that the filter performs as designs and removes unwanted noise.

Figure 4.2 shows results for the down-conversion and BB filtering portion of the frontend process. The top row of figures are the received signal PSD after down-conversion process and the BB filter response. Note that the top-left figure shows that down conversion is operating correctly in the simulation. The figure correctly shows that the signal PSD after the RF filter is now centered at baseband with spectral replicas appearing at $\pm 2 \times fc$ and having one-half the PSD magnitude. The BB filter, as mentioned in Section 3.1, is a 2nd-order Butterworth filter. The bottom plots in Figure 4.2 are the received signal PSD after BB filtering and the received signal after the frontend process. Note the before and after BB filtered PSD of the

down-converted signal. The after-picture reveals the filtered down converted signal without the higher frequency components. The PSD after BB filtering shows only the PSD centered around 0 Hz. This result indicates that the filter performed as designed by removing the unwanted components. The lower right-hand plot in Figure 4.2 shows approximately the same 31-Gold coded RBW as constructed (Figure 3.4) before carrier modulation. This final figure demonstrates that the conditioning process does perform successfully in removing channel noise and removing the carrier frequency.

4.1.2   Correlation Methods - Varying Sample Delay N_d.   The correlation methods discussed in Section 3.3 have three variables that are under the user's control for each signal type. The three variables are the correlation window width N_w, the signal delay N_d, and the step size between correlation iterations Δw. For ease of data presentation and comprehension, two of the three variables are held fixed. So for this research, N_d is varied while N_w and Δw are held constant. Note Δw controls the resolution of the output data. For best resolution, Δw is set to the smallest value of $\Delta w = 1$ for this work. For verification with the RBW signal, N_w is set equal to one full period of the RBW, or 1550 samples. The results for correlation methods A and B when varying N_d are provided in the following subsections.

4.1.2.1   Correlation-A with 31-Gold Code RBW Signal.   Results for the Correlation-A method using the 31-Gold coded RBW signal when varying N_d are shown in Figure 4.3. This figure represents the 'varying' reference correlation approach where $N_w = 1550$ samples and $\Delta w = 1$. By varying N_d (y-axis), correlation is done as describe in Section 3.3. The correlation window of 1550 samples is shifted by 1 between iterations and repeated for all the delay values. The correlation output for various delays values constructs the data matrix shown in Figure 4.3. Recall from Section 3.2 that the input RBW signal is periodic every 1550 samples. This explains the characteristic correlation peaks appearing in Figure 4.3 at shift values equaling integer multiples of 1550 samples (Delay = 0 and Delay = 1550). The max peaks represent the autocorrelation value. These results are consistent with the model and
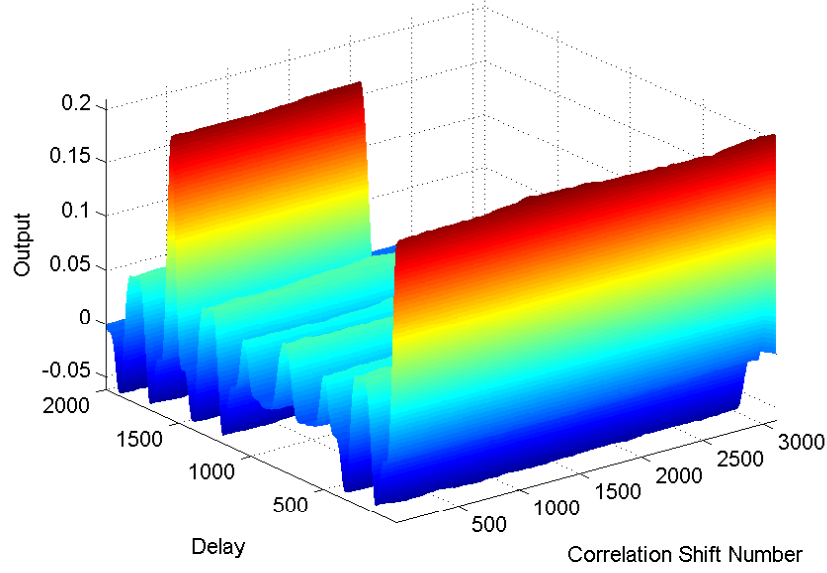
46

Figure 4.3:   Correlation-A output for RBW signal

the periodic 31-Gold coded RBW signal. The plots in Figure 4.4 are the data cuts for when N_d equals 1 and 500. Note the amplitude and consistency in the outputs regardless of the correlation shift numbers.

The surface plot in Figure 4.5 is the same correlation result but put on a normalized-dB scale. The plots in Figure 4.6 are the data cuts for when N_d equals 1 and 500. Note the amplitude and consistency in the outputs for all correlation shift numbers. These results validate that the system model using Correlation A is operating as designed. In terms of potential navigation, the correlation peak appearing for $N_d = 1550 \times n$ for $n = 0, 1, 2...$ gives reason to believe that the 31-Gold coded RBW signal does have 'promising' potential for navigation using the 'varying' reference Correlation A. Every autocorrelation peak is distinguishable and independent of the correlation shift number (i.e., arbitrary segment selection).

4.1.2.2   *Correlation-B with 31-Gold Code RBW Signal.*   Results for Correlation B method using the 31-Gold coded RBW signal are shown in Figure 4.7. This figure represents the 'fixed' reference correlation approach where $N_w = 1550$

Figure 4.4:   Correlation-A outputs for N_d equal 1 and 500
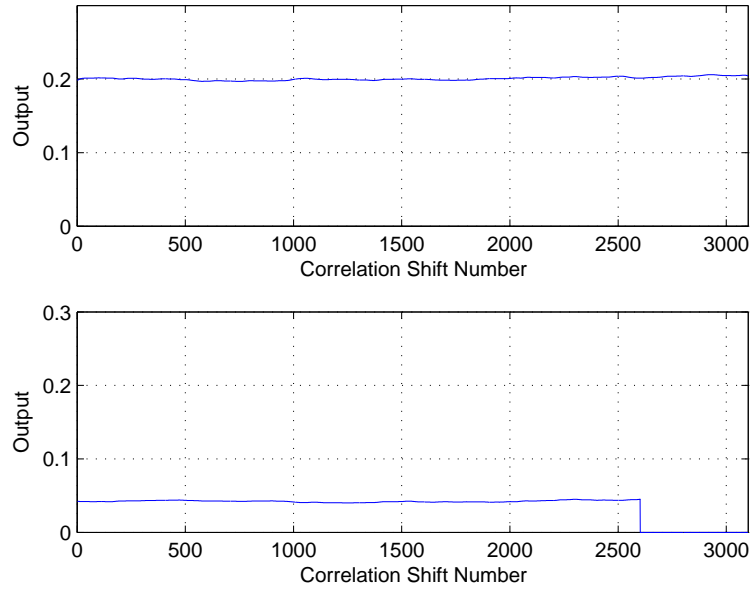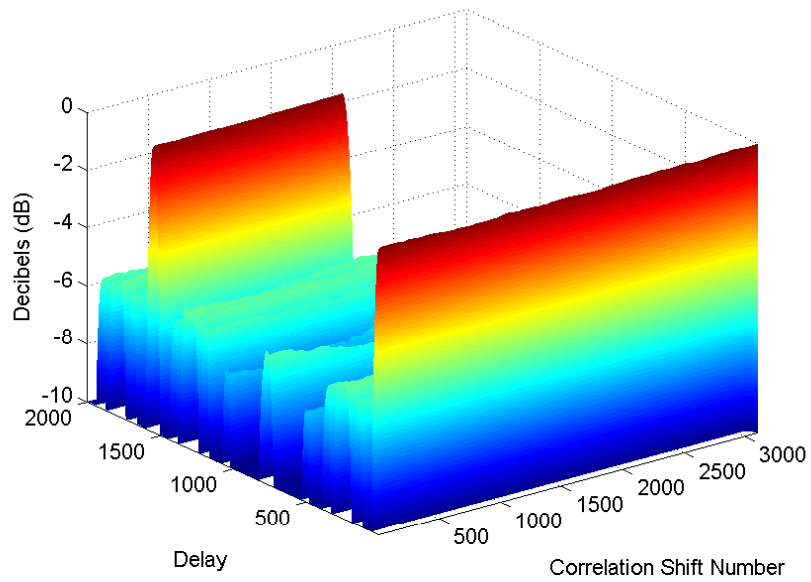

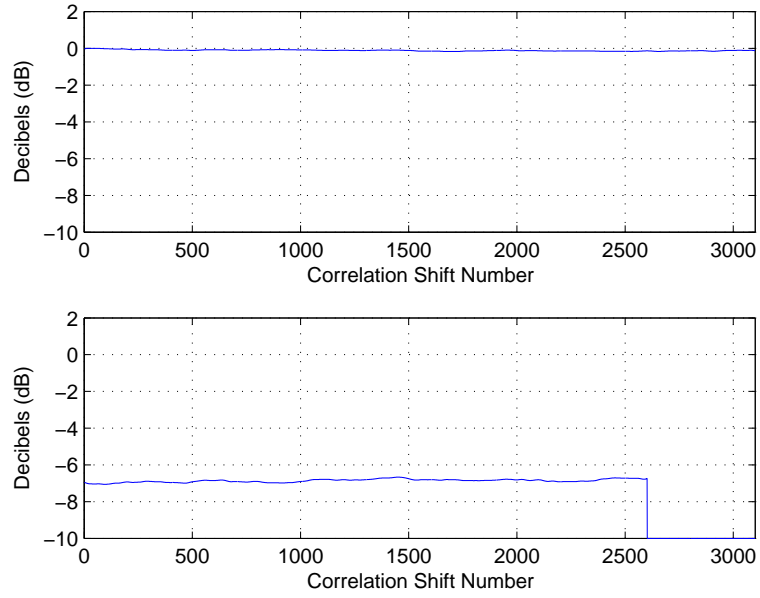Figure 4.5:   Magnitude of Correlation-A output (dB scale) for RBW signal

Figure 4.6: Magnitude of Correlation-A outputs (dB scale) for N_d equal 1 and 500
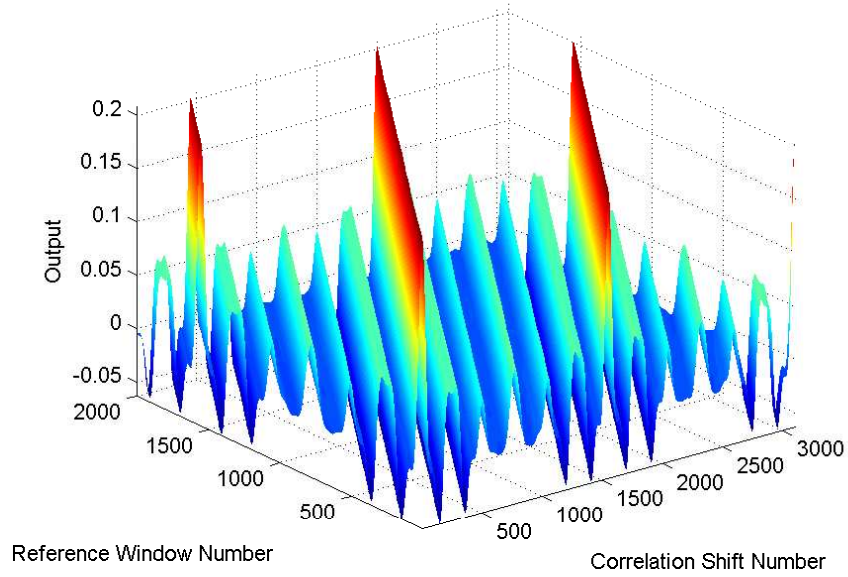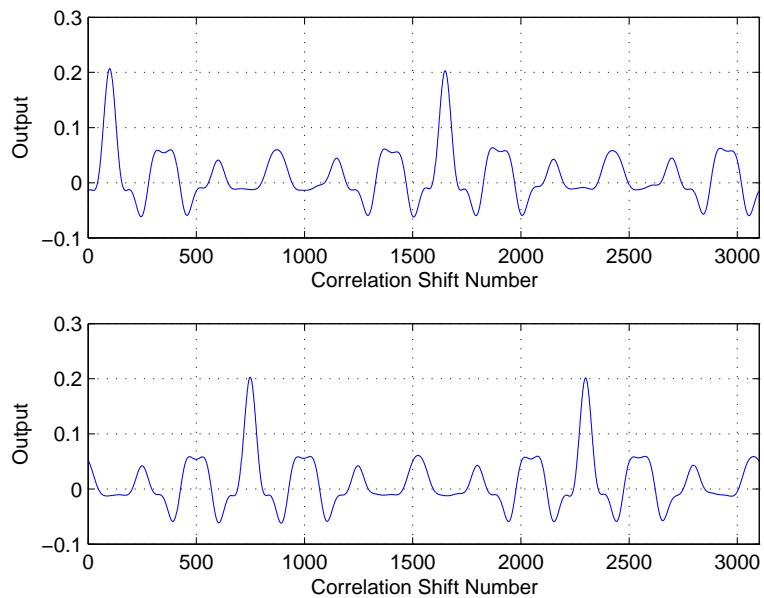

Figure 4.7: Correlation-B output for RBW signal

49

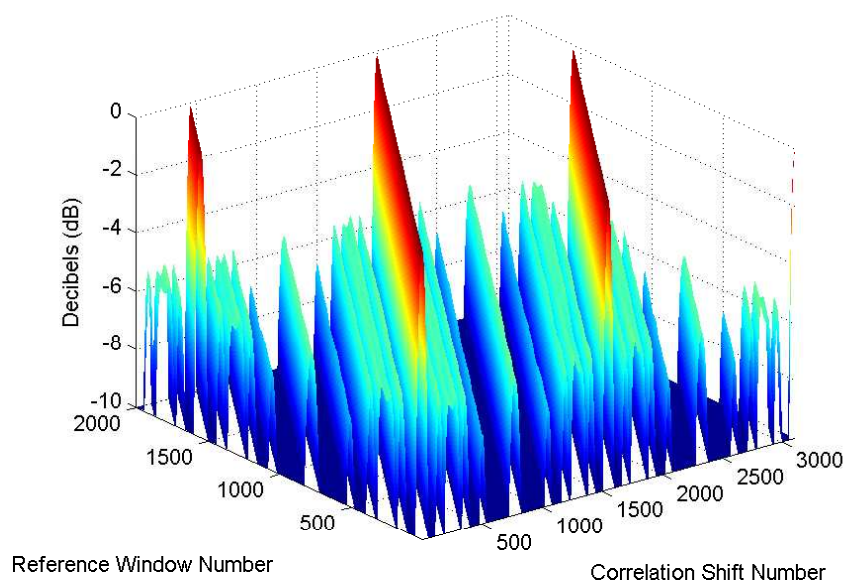Figure 4.8:   Correlation-B outputs for 100th and 749th reference window

Figure 4.9:   Magnitude of Correlation-B output (dB scale) for RBW signal
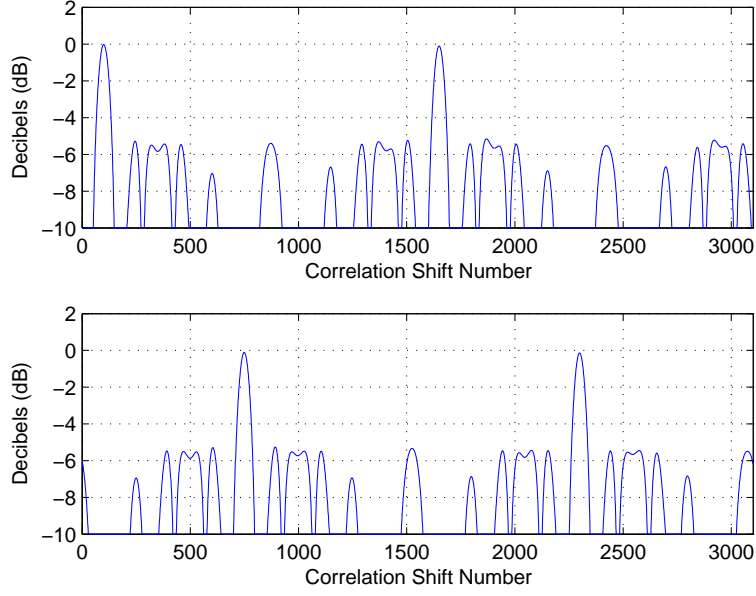
50

Figure 4.10:   Magnitude of Correlation-B outputs (dB scale) for 100th and 749th reference window

samples and $\Delta w = 1$. By varying N_d (y-axis), correlation is done as describe in Section 3.3. A correlation window of 1550 samples is shifted by 1 between iterations and repeated for every delay. The correlation output for various delays values constructs the data matrix shown in Figure 4.7. Recall from Section 3.2 that the input signal is a periodic signal every 1550 samples. This characteristic explains the diagonal correlation peaks across the data matrix. For every reference window number, the autocorrelation peak exists for the corresponding correlation shift number. The peak is periodic every 1550 samples as shown in Figure 4.8. The plots in Figure 4.8 are the data cuts for when N_d equals 100 and 749. These reference window numbers were selected as the largest and smallest autocorrelation peak. The two figures do not look much different and appear to be just shifted versions of each other. However, there is a slight difference in peak value. This will become more apparent in other cases. The structure in these plots is 100% consistent with the RBW input signal characteristics. The max peaks represent the autocorrelation value. The top figure is the correlation waveform for the 100th reference window number across all correlation

51

shift iterations. Note the peaks occurring every 1550 samples starting from the 100th correlation shift number. The bottom figure is the same correlation but using the 749th reference window. Note the peaks occurring every 1550 samples starting from the 749th correlation shift number. It is also important to note that the non-peak responses are effectively three-valued, which is consistent with the three-valued cross-correlation characteristics inherent in RBWs. These results are consistent with the model and the periodic 31-Gold coded RBW signal.

The surface plot in Figure 4.9 is the same correlation result but put on a normalized-dB scale. The plots in Figure 4.10 are the data cuts for when N_d equals 100 and 749. Note the amplitude and consistency in the outputs for all correlation shift numbers. These results validate that the system model using Correlation B is operating as designed. In terms of potential navigation, the correlation peak appears for all values N_d for some correlation shift number, regardless of which reference window used. The property suggests that the 31-Gold coded RBW signal has 'promising' potential for navigation using the 'fixed' reference Correlation B. Every autocorrelation peak is distinguishable and independent of the reference correlation number (i.e., arbitrary segment selection).

4.1.3 Correlation Methods - Varying Correlation Window Size N_w. For ease of data presentation and comprehension, two of three controllable variables in the correlation methods are held fixed. As mentioned before, the value for N_d is varied while N_w and Δw are held constant for this research. Note Δw controls the resolution of the output data and for best resolution, Δw is set to the smallest value which is 1. The N_w is set to one full period which is 1550 samples however for non-periodic signals, an optimum window size needs to be determined. So the following results tested what would happen if N_w were varied instead of N_d. The results for correlation methods A and B when varying N_w are shown below. Notice that only results for the 31-Gold coded RBW signal when varying correlation window size are shown. The simulations for all the other signals were performed with a majority of
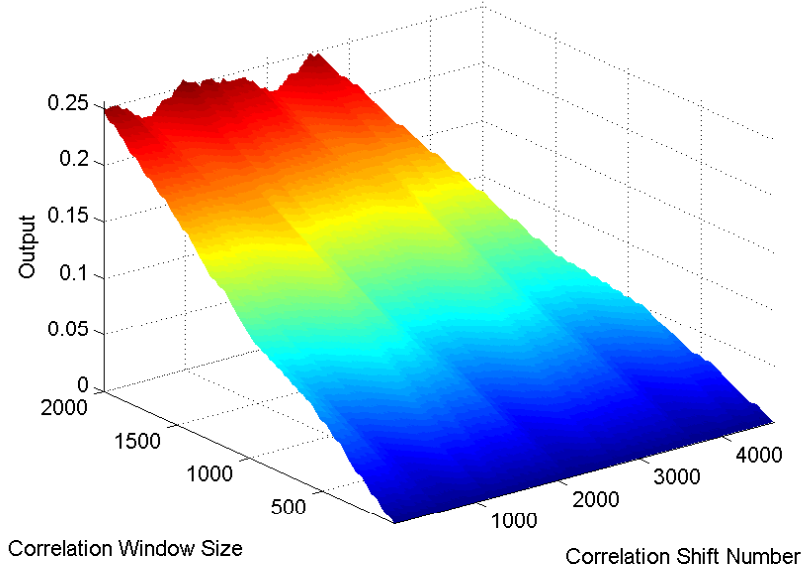
Figure 4.11:   Correlation-A output for RBW signal when varying N_w

the results showing the same overall trend. After this section, the remainder of the research and results presented herein only deal with the correlation methods having varying delay and not window sizes. For this research, the correlation window sizes were selected to be large enough to give meaningful results.

4.1.3.1 Correlation-A with 31-Gold Code RBW Signal. Results for Correlation A using the 31-Gold coded RBW signal when varying N_w is shown in Figure 4.11. This figure represents the 'varying' reference correlation approach where $N_d = 10$ samples and $\Delta w = 1$. By varying N_w (y-axis), correlation is done as describe in Section 3.3. The correlation window size is varied and is shifted by 1 sample between iterations and repeated for all the correlation window sizes. The correlation output for various window sizes constructs the data matrix shown in Figure 4.11. The variable N_d was set to 10 samples because this case showed the overall trend the best. Figure 4.11 shows that for correlation method A, larger windows correspond to larger correlation amplitudes. So the selection of $N_w = 1550$ was a workable value and provided adequate results. Remember from Section 2.2 that, in general, the larger

Table 4.2: N_w and Δw Values of Correlation-A

Signal Type	N_w	Δw
31-Gold coded RBW	1550	1
AM Song	1000	1000
AM Voice	1000	1000
FM Song	1000	1000
FM Voice	1000	1000
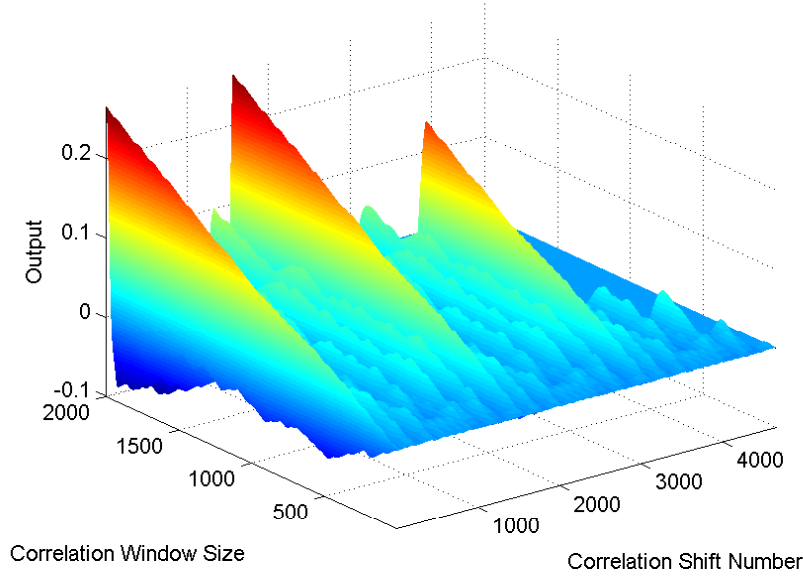
Figure 4.12:   Correlation-B output for RBW signal when vary-
ing N_w

the correlation window, a better correlation value will be given. This characteristic
explains the increasing correlation output peak value as the correlation window size
increases. There is a direct connection between the size of the correlation window and
the amplitude of the autocorrelation peak. So as long as the results were meaningful,
the user may use any correlation window size. The values for N_w and Δw used for
correlation method A are summarized in Table 4.2.

4.1.3.2   Correlation-B with 31-Gold Code RBW Signal.   The result for
the Correlation-B method using the 31-Gold coded RBW signal when varying N_w is
shown in Figure 4.12. This figure represents the 'fixed' reference correlation approach

54

Table 4.3: N_w and Δw Values of Correlation-B

Signal Type	N_w	Δw
31-Gold coded RBW	1550	1
AM Song	1000	1
AM Voice	1000	1
FM Song	1000	1
FM Voice	1000	1

where $N_d = 10$ samples and $\Delta w = 1$. By varying N_w (y-axis), correlation is done as describe in Section 3.3. The correlation window size is varied and is shifted by 1 sample between iterations and repeated for all the correlation window sizes. The correlation output for various window sizes constructs the data matrix shown in Figure 4.12. The variable N_d was set to 10 samples because this case showed the overall trend the best. Figure 4.12 shows that for correlation method B, larger windows correspond with larger correlation amplitude. So the selection of $N_w = 1550$ was a workable value. This characteristic explains the increasing correlation output peak value as the correlation window size increase. There is a direct connection between the size of the correlation window and the amplitude of the autocorrelation peak. So as long as the results were meaningful, the user may use any correlation window size. The values for N_w and Δw used for correlation method B are summarized in Table 4.3.

4.2   AM Radio Signal

The results shown in this section are for the AM radio signal. The results are organized by frontend results, Correlation-A results with song and voice signals, and Correlation-B results with song and voice signals. The frontend results are shown to verify that the signal out of the BB filter is the desired signal. The correlation results are shown by varying the signal delay. The results for the correlation process are organized into three plots. The first plot is the raw correlation data. The second plot is the normalized-dB scaled correlation data. And the last plot takes the cuts from the largest and smallest autocorrelation peak of the normalized-dB scaled data. The results are repeated for each correlation method and each signal data type.
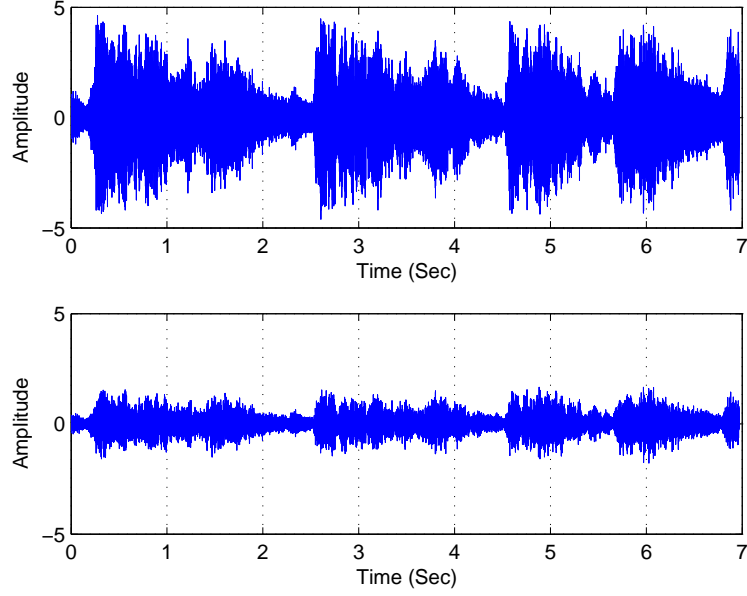
Figure 4.13: Conditioned AM song signal - Received (top) and Down-Converted (bottom) signal

4.2.1 AM Song Signal Results and Analysis. There are two types of data signals used in this research. The two data types are song and voice. The following results deal with the AM song signal as the input to the system model.

4.2.1.1 Frontend Process Results for AM Song Results. Figure 4.13 verifies that the frontend process is operating correctly. The top plot in Figure 4.13 is the received AM song signal where the bottom plot is the down-converted output signal from the frontend process. The before and after plots shows what the received signal looks like without the channel noise and the carrier frequency. The conditioned signal is the signal used for correlation.

4.2.1.2 Correlation-A with AM Song Signal. The result for the Correlation-A method using the AM song signal when varying N_d is shown in Figure 4.14. This figure represents the 'varying' reference correlation approach where $N_w = 1000$ samples and $\Delta w = 1000$. The Δw is set to 1000 samples to simulate a real-time process. By varying N_d (y-axis), correlation is done as describe in Section 3.3. The correlation
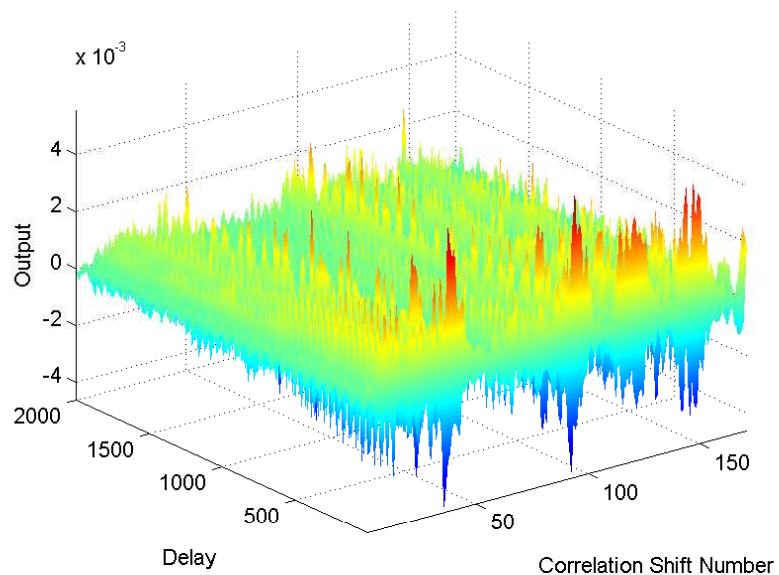
56

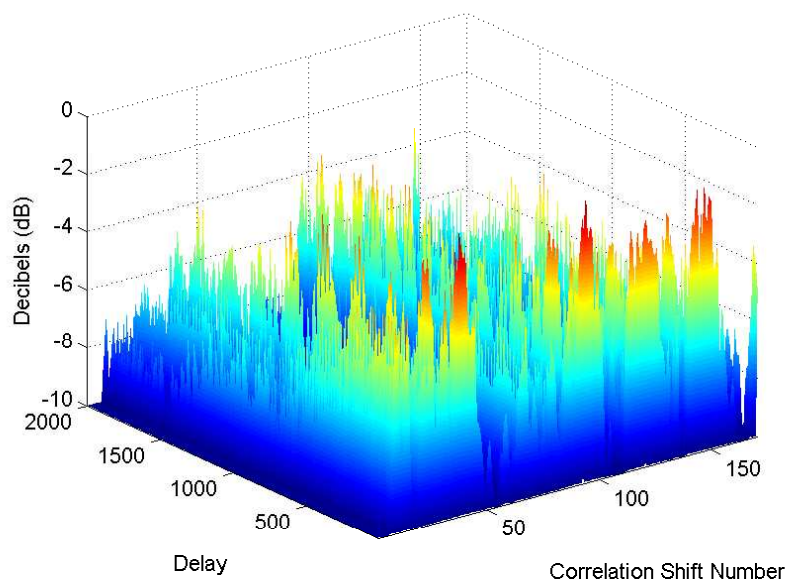Figure 4.14:   Correlation-A output for AM song signal

Figure 4.15:   Magnitude of Correlation-A output (dB scale) for AM song signal
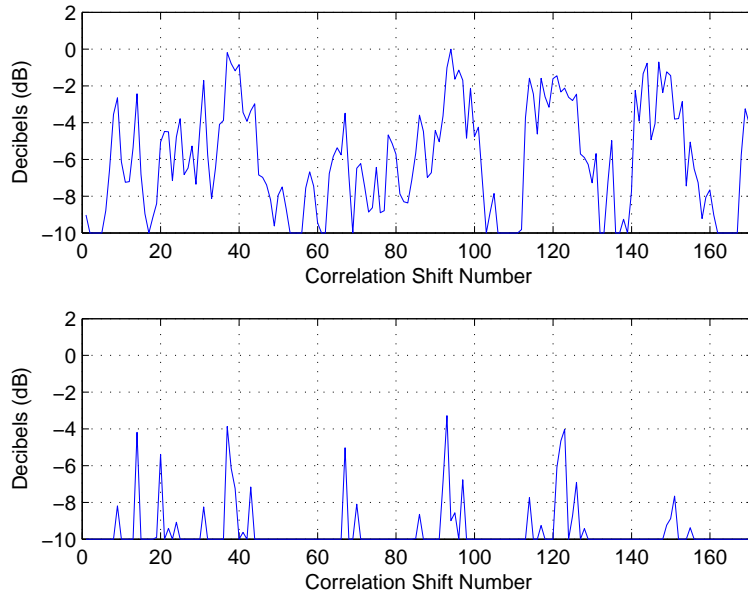
Figure 4.16:   Magnitude of Correlation-A outputs (dB scale)
for 1st and 500th reference window

window of 1000 samples is shifted by 1000 between iterations and repeated for all
the delay values. The correlation output for various delays values constructs the data
matrix shown in Figure 4.14. The max peaks are suppose to represent the autocor-
relation value. This plot does have distinguished max peaks. The max peaks occur
when $N_d = 0$ which makes sense since this is the definition of autocorrelation.

The surface plot in Figure 4.15 is the same correlation result but put on a
normalized-dB scale. Putting the data on a dB-scale provides another comparison by
looking at relative power. The plots in Figure 4.16 are the data cuts for when N_d
equals 1 and 500. Note the varying amplitudes within each plot and the difference in
amplitude between the plots. The correlation peak only appears sporadically when
$N_d = 0$. And when $N_d = 0$, the magnitude of the autocorrelation peak varies and is
now dependent on the correlation shift number. This inconsistent trend gives reason
to believe that the AM song signal only has 'limited' potential for navigation using
the 'varying' correlation method A. A distinguishable autocorrelation peak does not
occur for every arbitrary segment selection.
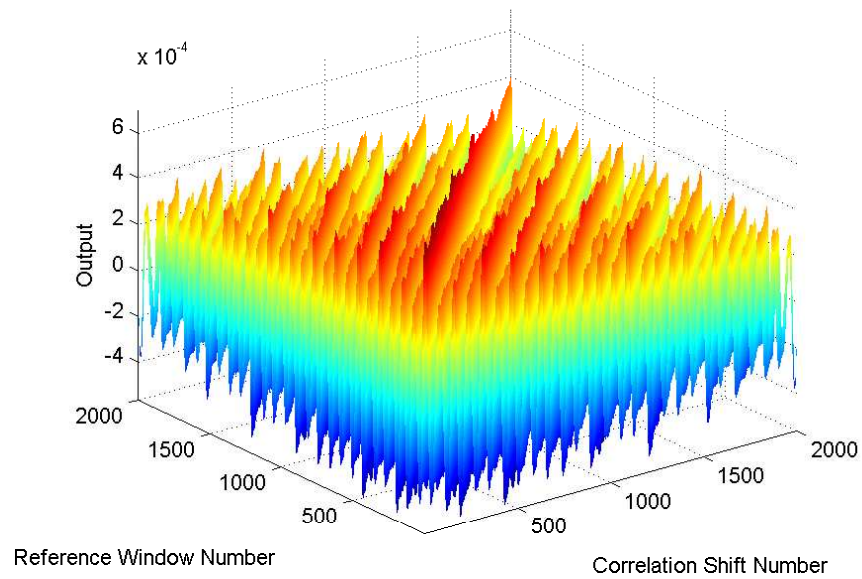
58

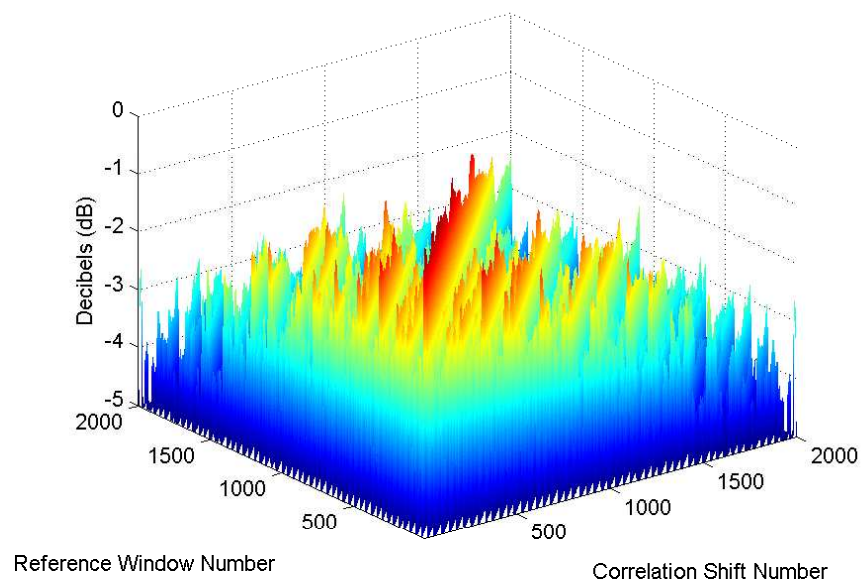Figure 4.17:   Correlation-B output for AM song signal

Figure 4.18:   Magnitude of Correlation-B output (dB scale)
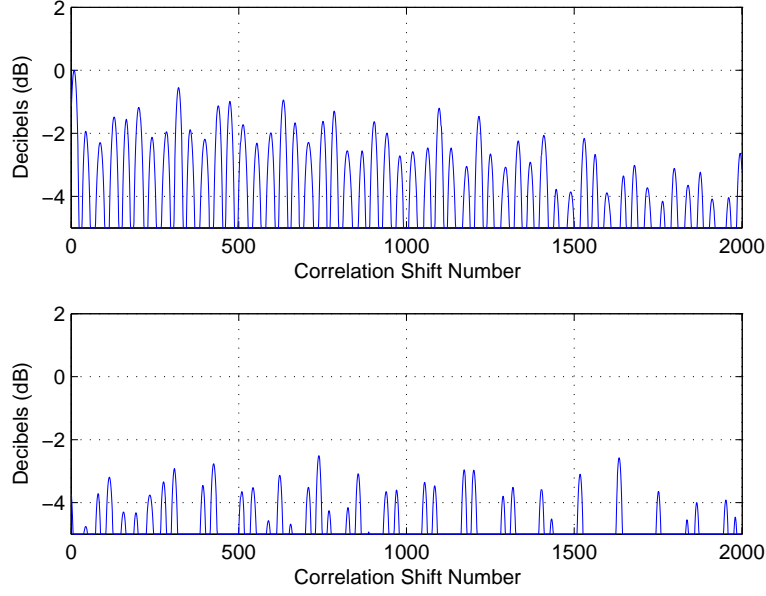for AM song signal

Figure 4.19:   Magnitude of Correlation-B outputs (dB scale)
for 9th and 1635th reference window

4.2.1.3   Correlation-B with AM Song Signal.   The result for the Correlation-
B method using the AM song signal is shown in Figure 4.17. This figure represents
the 'fixed' reference correlation approach where $N_w = 1000$ samples and $\Delta w = 1$.
By varying N_d (y-axis), correlation is done as describe in Section 3.3. A correlation
window of 1000 samples is shifted by 1 between iterations and repeated for every ref-
erence window number. The correlation output for various delay values constructs the
data matrix shown in Figure 4.17. For every reference window, the autocorrelation
peak exists for the corresponding correlation shift number. The autocorrelation peak
is expected to be seen on the diagonal of the data matrix. However there are other
peaks not on the diagonal that are relatively close in amplitude.

The surface plot in Figure 4.18 is the same correlation result but put on a
normalized-dB scale. Putting the data on a dB-scale provides another comparison by
looking at relative power. The plots in Figure 4.19 are the data cuts for when N_d
equals 9 and 1635. These reference window numbers were selected as the largest and
smallest autocorrelation peak. Note the varying amplitudes within each plot and the
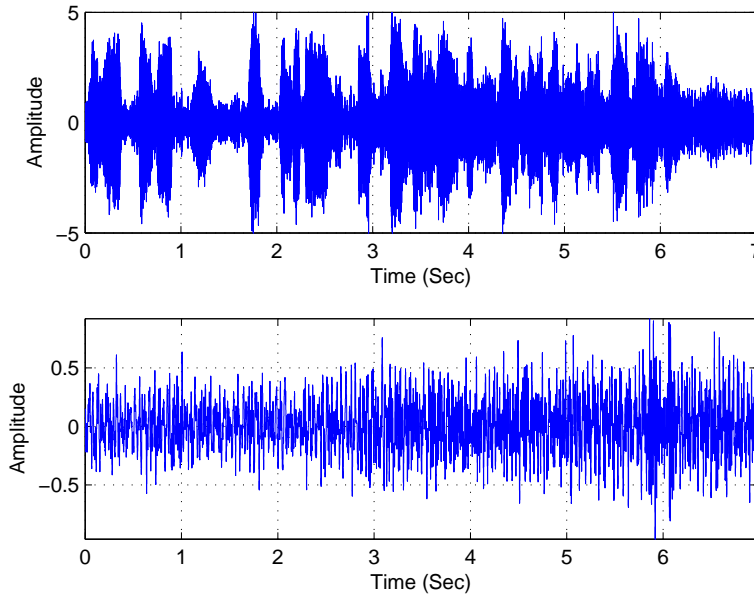
60

Figure 4.20:   Conditioned AM voice signal - Received (top) and Down-Converted (bottom) signal

difference in amplitude between the plots. In terms of potential navigation, the actual autocorrelation peak is difficult to identify because there are too many peaks within 2dB of each other. This undistinguishable result gives reason to believe that the AM song signal only has 'limited' potential for navigation using the 'fixed' correlation method B. An autocorrelation peak does occur for every arbitrary segment selection but it is not definitely distinguishable.

4.2.2   AM Voice Signal Results and Analysis.   There are two types of data signals used in this research. The two data types are song and voice. The following results deal with the AM voice signal as the input to the system model.

4.2.2.1   Frontend Process Results for AM Voice Results.   Figure 4.20 verifies that the frontend process is operating correctly. The top plot in Figure 4.20 is the received AM voice signal where the bottom plot is the down-converted output signal from the frontend process. The before and after plots shows what the received
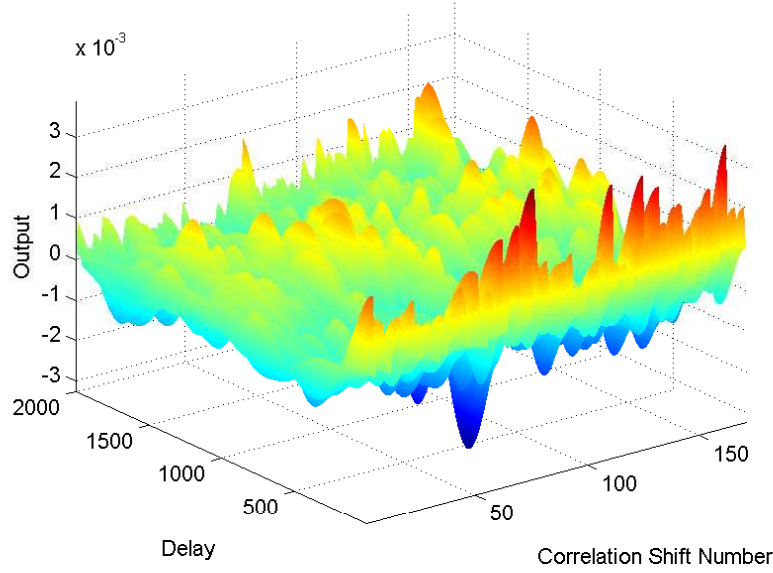
Figure 4.21:   Correlation-A output for AM voice signal

signal looks like without the channel noise and the carrier frequency. The conditioned signal is the signal used for correlation.

4.2.2.2 Correlation-A with AM Voice Signal.   The result for the Correlation-A method using the AM voice signal when varying N_d is shown in Figure 4.21. This figure represents the 'varying' reference correlation approach where $N_w = 1000$ samples and $\Delta w = 1000$. The Δw is set to 1000 samples to simulate a real-time process. By varying N_d (y-axis), correlation is done as describe in Section 3.3. The correlation window of 1000 samples is shifted by 1000 between iterations and repeated for all the delay values. The correlation output for various delays values constructs the data matrix shown in Figure 4.21. The max peaks are suppose to represent the autocorrelation value. This plot does have distinguished max peaks. The max peaks occur when $N_d = 0$ which makes sense since this is the definition of autocorrelation.

The surface plot in Figure 4.22 is the same correlation result but put on a normalized-dB scale. Putting the data on a dB-scale provides another comparison be
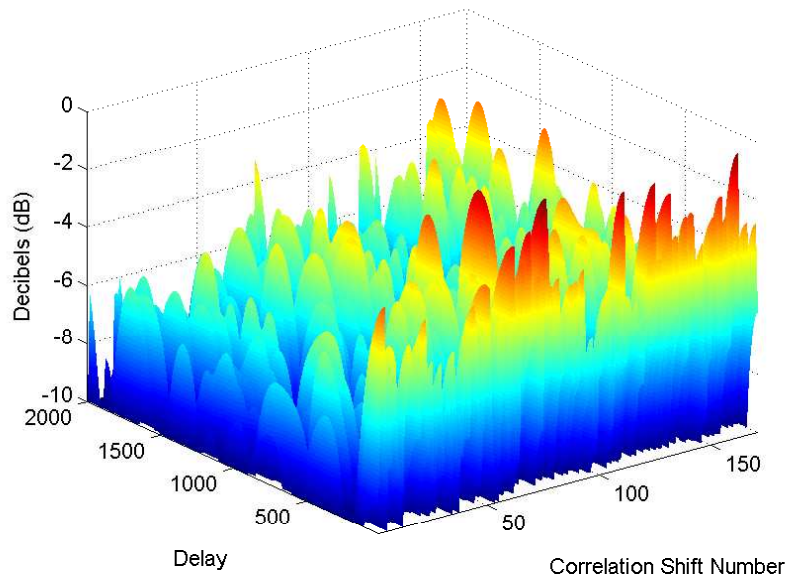
62

Figure 4.22: Magnitude of Correlation-A output (dB scale) for AM voice signal
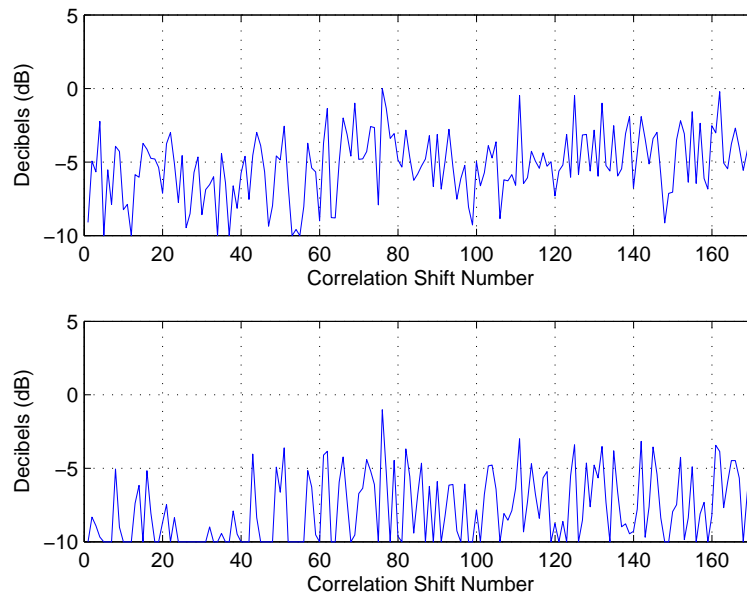

Figure 4.23: Magnitude of Correlation-A outputs (dB scale) for 1st and 500th reference window
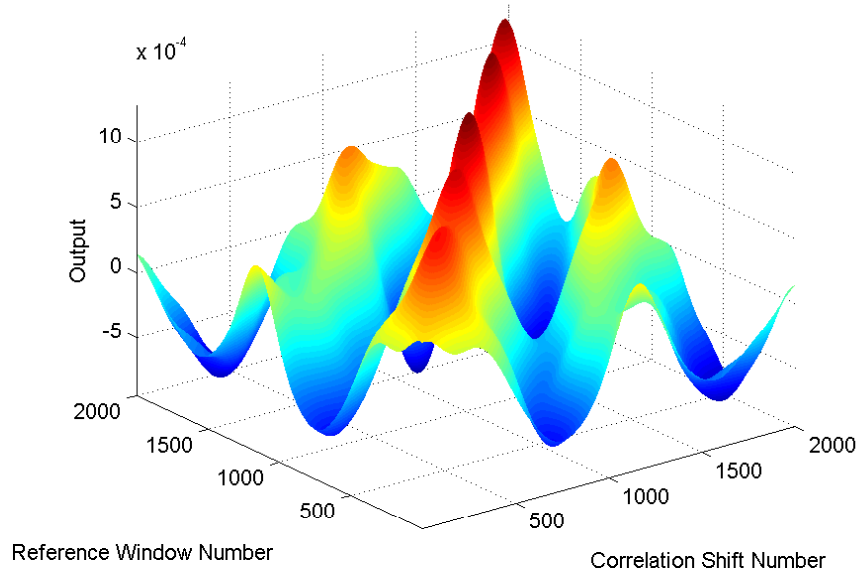
Figure 4.24:   Correlation-B output for AM voice signal

looking at relative power. The plots in Figure 4.23 are the data cuts for when N_d equals 1 and 500. Note the varying amplitudes within each plot and the difference in amplitude between the plots. The correlation peak appears sporadically throughout the matrix. Multiple peaks give reason to believe that the AM voice signal only has 'limited' potential for navigation using the 'varying' correlation method A. A distinguishable autocorrelation peak does not occur for every arbitrary segment selection.

4.2.2.3   Correlation-B with AM Voice Signal.   The result for the Correlation-B method using the AM song signal is shown in Figure 4.24. This figure represents the 'fixed' reference correlation approach where $N_w = 1000$ samples and $\Delta w = 1$. By varying N_d (y-axis), correlation is done as describe in Section 3.3. A correlation window of 1000 samples is shifted by 1 between iterations and repeated for every reference window number. The correlation output for various delays value constructs the data matrix shown in Figure 4.24. For every reference window, the autocorrelation peak exists for the corresponding correlation shift number. The auto-

64

Figure 4.25: Magnitude of Correlation-B output (dB scale) for AM voice signal

Figure 4.26: Magnitude of Correlation-B outputs (dB scale) for 1330th and 249th reference window
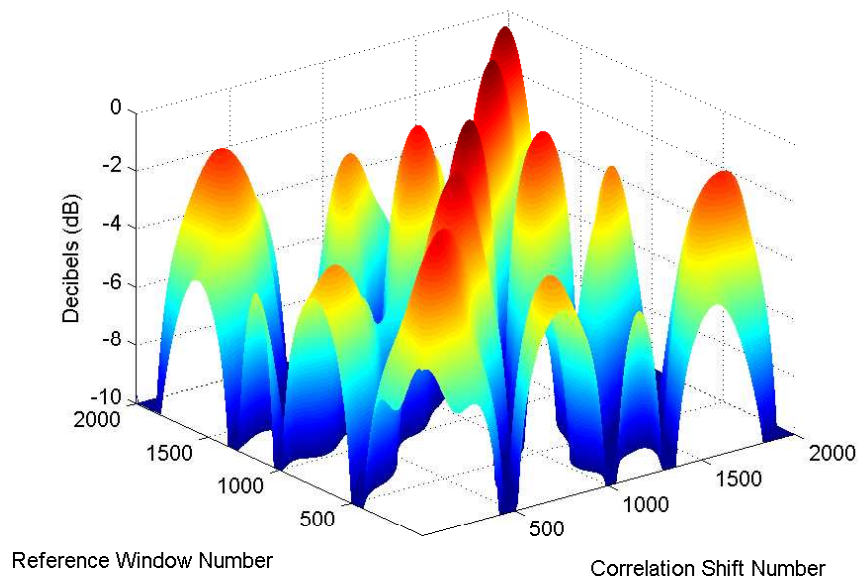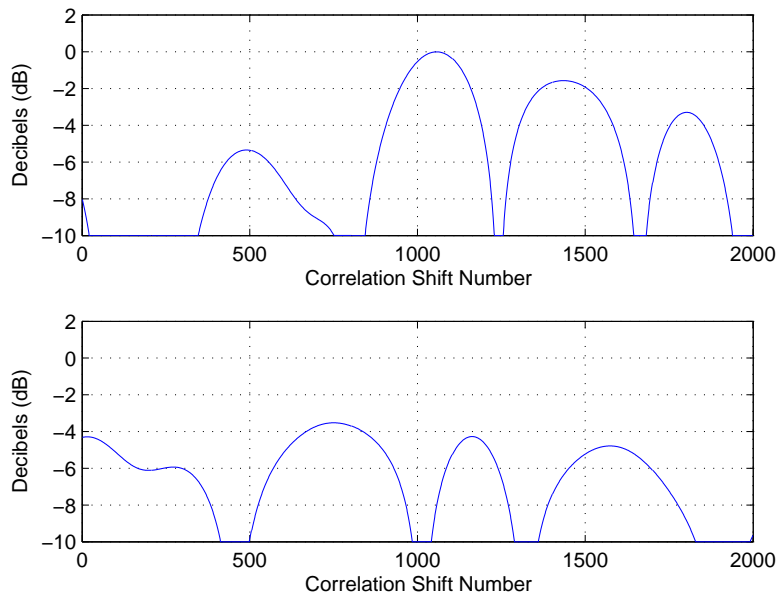
correlation peak is expected to be seen on the diagonal of the data matrix. However there are other peaks not on the diagonal that are relatively close in amplitude.

The surface plot in Figure 4.25 is the same correlation result but put on a normalized-dB scale. Putting the data on a dB-scale provides another comparison by looking at relative power. The plots in Figure 4.26 are the data cuts for when N_d equals 1330 and 249. These reference window numbers were selected as the largest and smallest autocorrelation peak. Note the varying amplitudes within each plot and the difference in amplitude between the plots. In terms of potential navigation, there are too many peaks within 2.0 dB of each other making it difficult to identify the actual autocorrelation peak. This undistinguishable result gives reason to believe that the AM voice signal only has 'limited' potential for navigation using the 'fixed' correlation method B. One distinguishable autocorrelation peak does not occur for every arbitrary segment selection.

4.3   FM Radio Signal

The results shown in this section are for the FM radio signal. The results are organized by frontend results, Correlation-A results with song and voice signals, and Correlation-B results with song and voice signals. The frontend results are shown to verify that the signal out of the BB filter is the desired signal. The correlation results are shown by varying the signal delay. The results for the correlation process are organized into three plots. The first plot is the raw correlation data. The second plot is the normalized-dB scaled correlation data. And the last plot takes the cuts from the largest and smallest autocorrelation peak of the normalized-dB scaled data. The results are repeated for each correlation method and each signal data type.

4.3.1   FM Song Signal Results and Analysis.   There are two types of data signals used in this research. The two data types are song and voice. The following results deal with the FM song signal as the input to the system model.
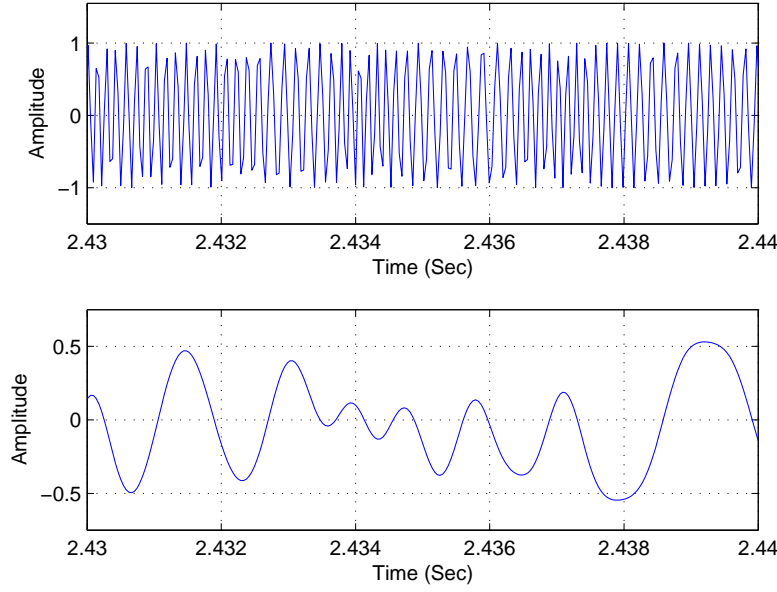
Figure 4.27:   Conditioned FM song signal - Received (top) and
Down-Converted (bottom) signal

4.3.1.1   Frontend Process Results for FM Song Results.   Figure 4.27
verifies that the frontend process is operating correctly. The top plot in Figure 4.27
is the received FM song signal where the bottom plot is the down-converted output
signal from the frontend process. The before and after plots shows what the received
signal looks like without the channel noise and the carrier frequency. The conditioned
signal is the signal used for correlation.

4.3.1.2   Correlation-A with FM Song Signal.   The result for the Correlation-
A method using the FM song signal when varying N_d is shown in Figure 4.28. This
figure represents the 'varying' reference correlation approach where $N_w = 1000$ sam-
ples and $\Delta w = 1000$. The Δw is set to 1000 samples to simulate a real-time process.
By varying N_d (y-axis), correlation is done as describe in Section 3.3. The correla-
tion window of 1000 samples is shifted by 1000 between iterations and repeated for
all the delay values. The correlation output for various delays values constructs the
data matrix shown in Figure 4.28. The max peaks are suppose to represent the au-
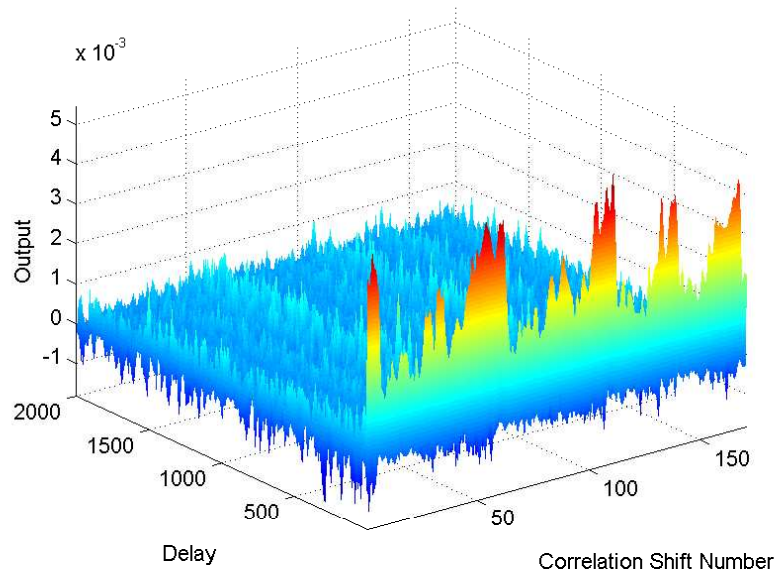tocorrelation value. This plot does have distinguished max peaks but the results are

67

Figure 4.28:   Correlation-A output for FM song signal

Figure 4.29:   Magnitude of Correlation-A output (dB scale)
for FM song signal

Figure 4.30: Magnitude of Correlation-A outputs (dB scale) for 1st and 500th reference window

somewhat inconsistent across the correlation shift number. This results means that there is not a guarantee of good CPI for any arbitrary segment of the signal.

The surface plot in Figure 4.29 is the same correlation result but put on a normalized-dB scale. Putting the data on a dB-scale provides another comparison by looking at relative power. The plots in Figure 4.30 are the data cuts for when N_d equals 1 and 500. Note the varying amplitudes within each plot and the difference in amplitude between the plots. The correlation peak appearing only when $N_d = 0$. And when $N_d = 0$, the magnitude of the autocorrelation peak varies and is now dependent on the correlation shift number. This gives reason to believe that the FM song signal only has 'limited' potential for navigation using the 'varying' correlation method A. A distinguishable autocorrelation peak does not occur for every arbitrary segment selection.

4.3.1.3 Correlation-B with FM Song Signal. The result for the Correlation-B method using the FM song signal is shown in Figure 4.31. This figure represents

69

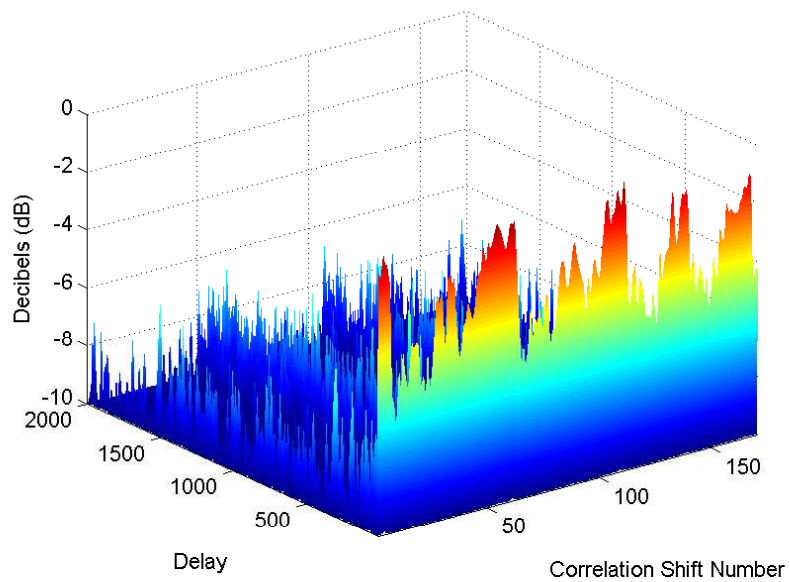Figure 4.31:   Correlation-B output for FM song signal

Figure 4.32:   Magnitude of Correlation-B output (dB scale) for FM song signal
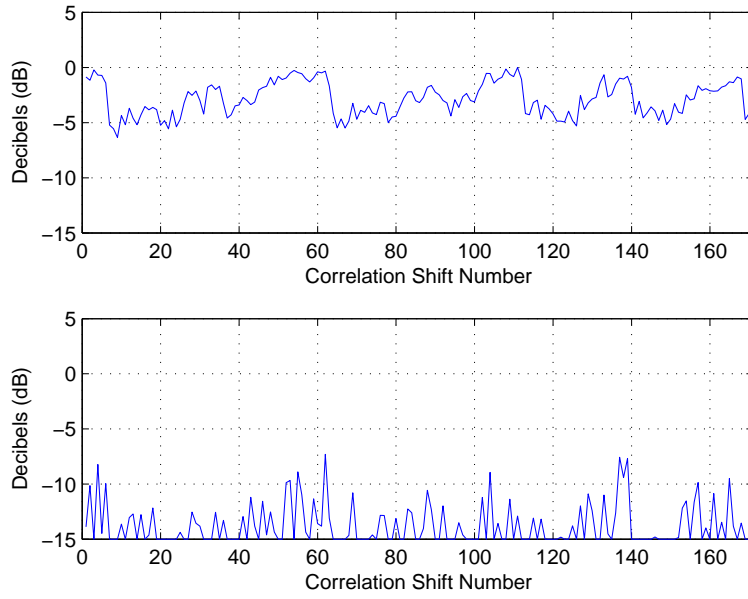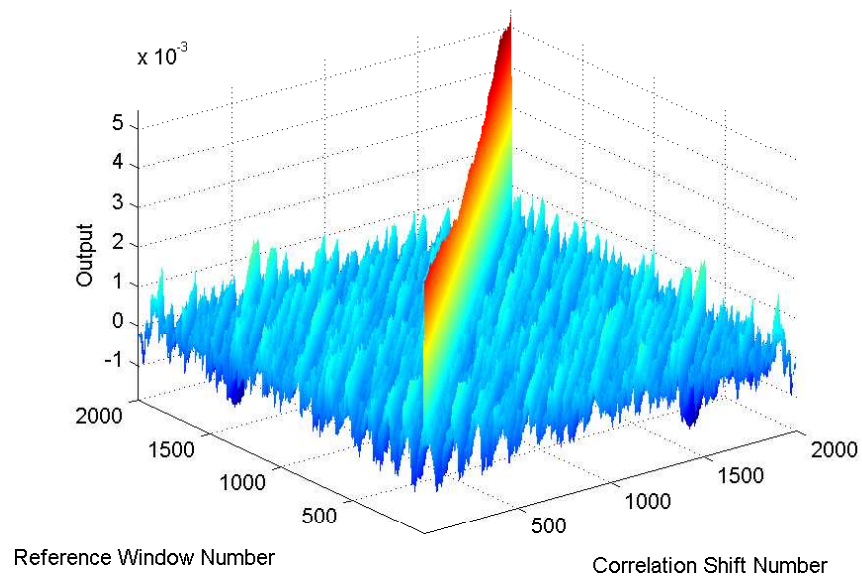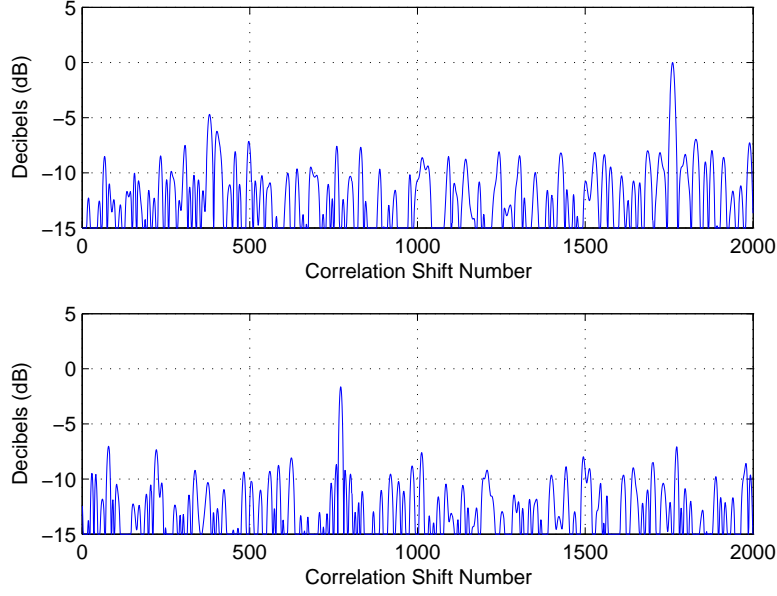
Figure 4.33:   Magnitude of Correlation-B outputs (dB scale)
for 1761st and 772th reference window

the 'fixed' reference correlation approach where $N_w = 1000$ samples and $\Delta w = 1$.
By varying N_d (y-axis), correlation is done as describe in Section 3.3. A correlation
window of 1000 samples is shifted by 1 between iterations and repeated for every
reference window number. The correlation output for various delay values constructs
the data matrix shown in Figure 4.31. For every reference window, the autocorrela-
tion peak exists for the corresponding correlation shift number. The autocorrelation
peak is expected to be seen on the diagonal of the data matrix. This case has a very
distinguished correlation peak for each reference window number.

The surface plot in Figure 4.32 is the same correlation result but put on a
normalized-dB scale. Putting the data on a dB-scale provides another comparison by
looking at relative power. The plots in Figure 4.33 are the data cuts for when N_d
equals 1761 and 772. These reference window numbers were selected as the largest and
smallest autocorrelation peak. Note the varying amplitudes within each plot and the
difference in amplitude between the plots. In terms of potential navigation, there is a
5.0 dB difference between the peak and sidelobes which makes it easy to identify the
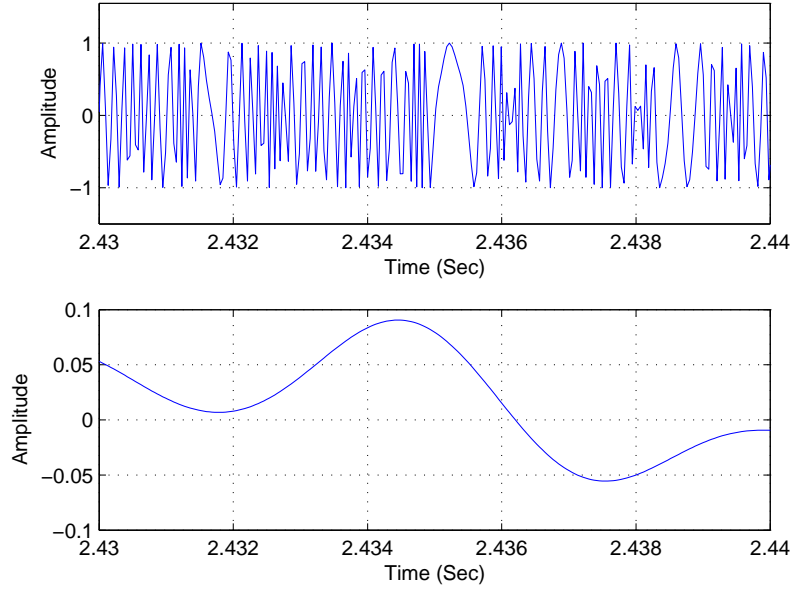
Figure 4.34:   Conditioned FM voice signal - Received (top) and Down-Converted (bottom) signal

autocorrelation peak. This definite result gives reason to believe that the FM song signal has 'promising' potential for navigation using the 'fixed' correlation method B. Every autocorrelation peak is distinguishable and independent of the reference window number (i.e., arbitrary segment selection).

4.3.2   FM Voice Signal Results and Analysis.   There are two types of data signals used in this research. The two data types are song and voice. The following results deal with the FM voice signal as the input to the system model.

4.3.2.1   Frontend Process Results for FM Voice Results.   Figure 4.34 verifies that the frontend process is operating correctly. The top plot in Figure 4.34 is the received FM voice signal where the bottom plot is the down-converted output signal from the frontend process. The before and after plots shows what the received signal looks like without the channel noise and the carrier frequency. The conditioned signal is the signal used for correlation.

72
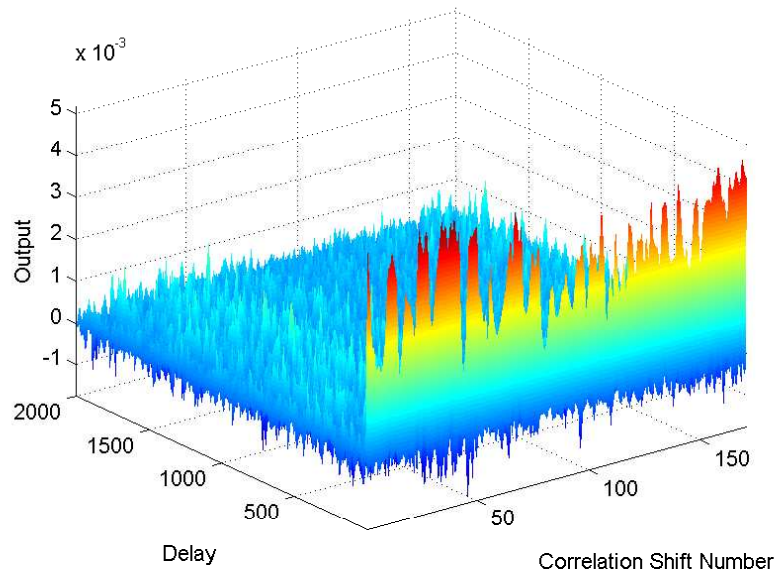
Figure 4.35:   Correlation-A output for FM voice signal

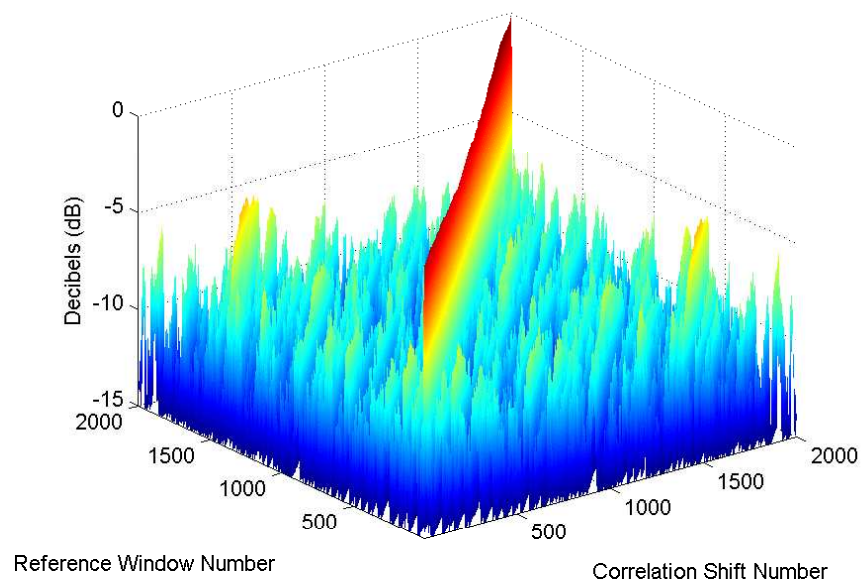Figure 4.36:   Magnitude of Correlation-A output (dB scale) for FM voice signal
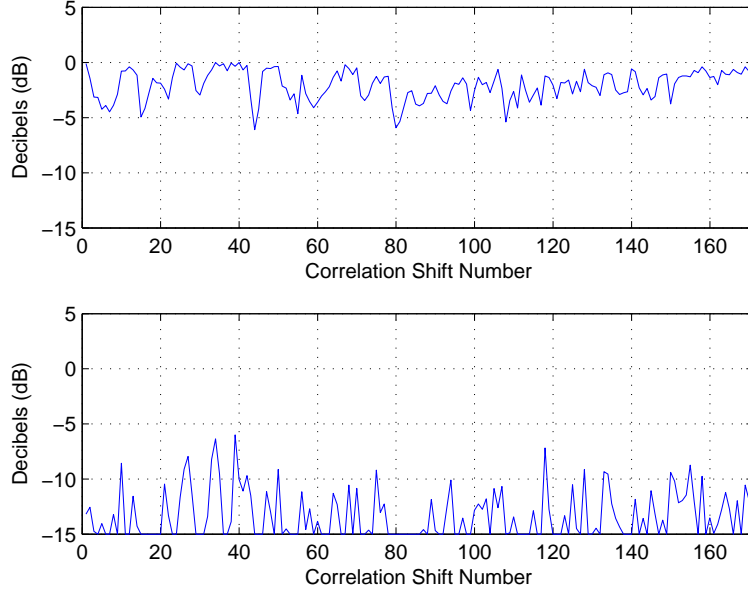
Figure 4.37:   Magnitude of Correlation-A outputs (dB scale)
for 1st and 500th reference window

4.3.2.2   Correlation-A with FM Voice Signal.   The result for the
Correlation-A method using the FM voice signal when varying N_d is shown in Figure 4.35. This figure represents the 'varying' reference correlation approach where
$N_w = 1000$ samples and $\Delta w = 1000$. The Δw is set to 1000 samples to simulate
a real-time process. By varying N_d (y-axis), correlation is done as describe in Section 3.3. The correlation window of 1000 samples is shifted by 1000 between iterations
and repeated for all the delay values. The correlation output for various delays values
constructs the data matrix shown in Figure 4.35. The max peaks are suppose to
represent the autocorrelation value. This plot does have distinguished max peaks.
The max peaks occur when $N_d = 0$ which makes sense since this is the definition of
autocorrelation.

The surface plot in Figure 4.36 is the same correlation result but put on a
normalized-dB scale. Putting the data on a dB-scale provides another comparison by
looking at relative power. The plots in Figure 4.37 are the data cuts for when N_d
equals 1 and 500. Note the varying amplitudes within each plot and the difference in

74
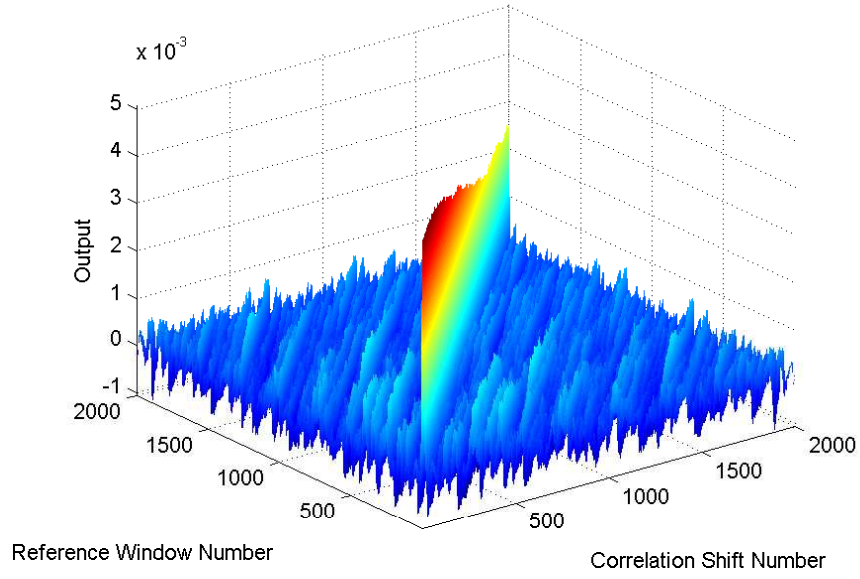
Figure 4.38: Correlation-B output for FM voice signal

amplitude between the plots. The correlation peak appearing only when $N_d = 0$. And when $N_d = 0$, the magnitude of the autocorrelation peak varies and is now dependent on the correlation shift number. This gives reason to believe that the FM voice signal only has 'limited' potential for navigation using the 'varying' correlation method A. A distinguishable autocorrelation peak does not occur for every arbitrary segment selection.

4.3.2.3 Correlation-B with FM Voice Signal. The result for the Correlation-B method using the FM song signal is shown in Figure 4.38. This figure represents the 'fixed' reference correlation approach where $N_w = 1000$ samples and $\Delta w = 1$. By varying N_d (y-axis), correlation is done as describe in Section 3.3. A correlation window of 1000 samples is shifted by 1 between iterations and repeated for every reference window number. The correlation output for various delays values constructs the data matrix shown in Figure 4.38. For every reference window, the autocorrelation peak exists for the corresponding correlation shift number. The au-
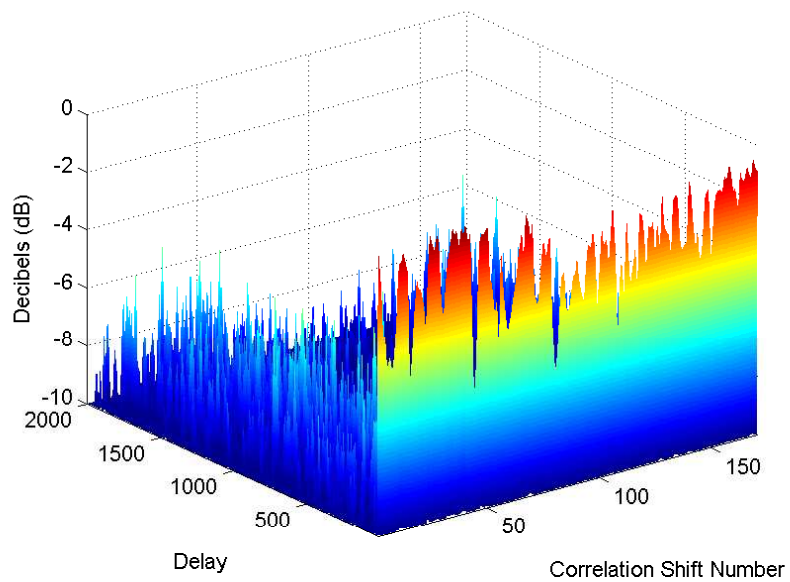
75
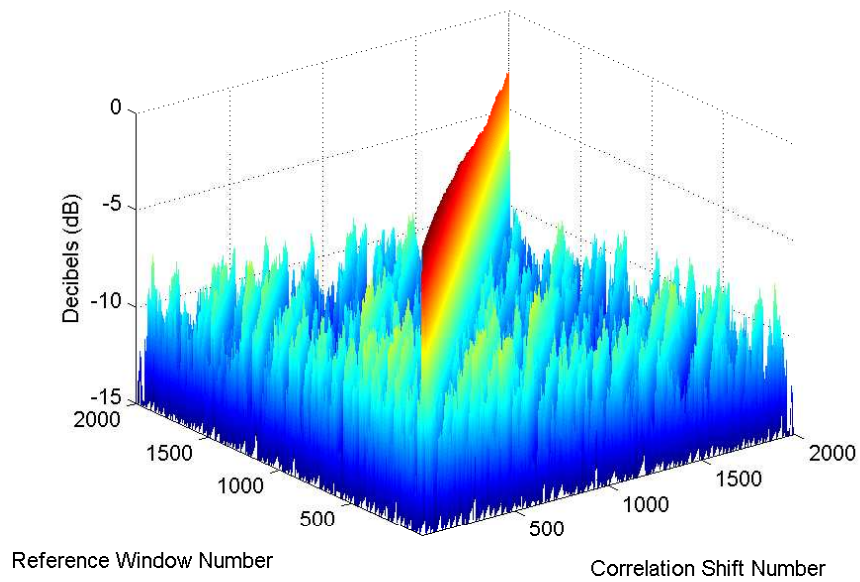
Figure 4.39: Magnitude of Correlation-B output (dB scale) for FM voice signal
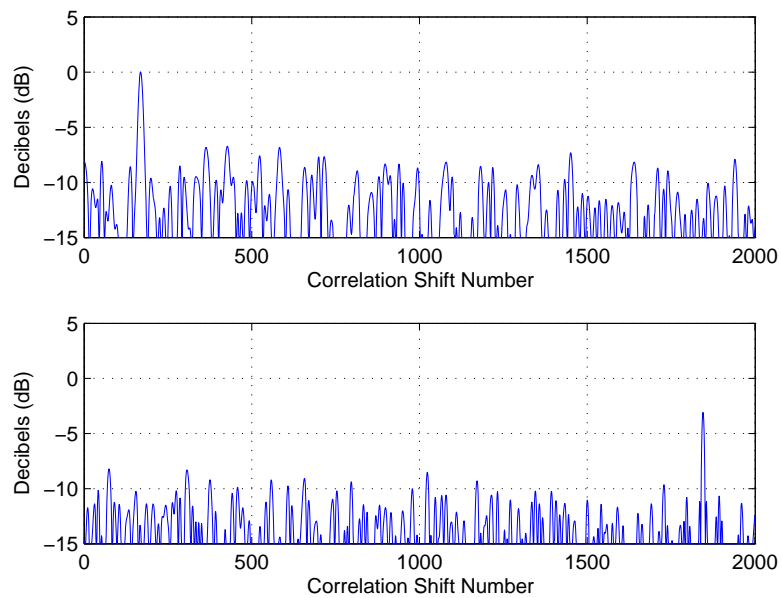
Figure 4.40: Magnitude of Correlation-B outputs (dB scale) for 169st and 1846th reference window

tocorrelation peak is expected to be seen on the diagonal of the data matrix. This case has a very distinguished correlation peak for each reference window number.

The surface plot in Figure 4.39 is the same correlation result but put on a normalized-dB scale. Putting the data on a dB-scale provides another comparison by looking at relative power. The plots in Figure 4.40 are the data cuts for when N_d equals 169 and 1846. These reference window numbers were selected as the largest and smallest autocorrelation peak. Note the varying amplitudes within each plot and the difference in amplitude between the plots. In terms of potential navigation, there is at least a 5.0 dB difference between the peak and sidelobes which makes it easy to identify the autocorrelation peak. This positive result gives reason to believe that the FM song signal has 'promising' potential for navigation using the 'fixed' correlation method B. Every autocorrelation peak is distinguishable and independent of the reference window number (i.e., arbitrary segment selection).

4.4   Summary

This chapter presented and analyzed results from simulations conducted with the receiver model and two correlation methods. The system model was validated by presenting and analyzing the simulation results for the 31-Gold Code RBW signal. The AM radio signals were used in the simulations, with all AM radio results showing 'limited' potential for navigation. However, the FM radio signals provided 'promising' results for both the voice and song data files considered. Only the correlation method B with both FM radio signals produced distinct autocorrelation peaks for all reference window numbers. The correlation peaks occur regardless of which window is used as a reference means that TDOA can be done with FM radio signals using the 'fixed' correlation method B. Using one reference receiver and two target receivers, TDOA can be used on the FM radio signal Correlation-B peaks to navigate. The FM radio signals showed 'limited' potential when using the 'varying' correlation method A.

V. Conclusions and Recommendations

This chapter summarizes the research results of the correlation receiver model and CPI/navigation potential of AM and FM radio signals. Recommendations for future research using AM and FM radio signals, as well as other signals, are also provided.

5.1 Summary of Results

The primary objective of this research was to determine the CPI of arbitrary AM and FM radio signals for the purpose of navigation. In support of this objective, this research investigated two separate correlation receiver methods can hopefully be used to produce desired autocorrelation peaks between the received signals of the reference and target receivers. This section summarizes the test results presented in Chapter IV.

5.1.1 Correlation Receiver Model Results. Two of three components of the correlation receiver (Figure 3.2) were modelled and performance simulated under this research. The components considered were the RF-IF frontend and the correlation processing. The RF-IF frontend process performed as it was designed. It effectively filters out unwanted noise and brought the input signal down to baseband frequency as seen in Figure 4.1 and Figure 4.2.

Two correlation methods were designed so that any generic signal can be analyzed as the input signal and not just the AM and FM radio signals considered here. Models for the two correlation methods were analyzed and verified by using an input signal having well-defined and known correlation characteristics. Using a well-known 31-Gold coded signal as the input signal, it was verified/validated that both correlation models performed as designed. For ease of presentation and discussion, one correlation technique is called *Correlation A* and produces results which are representative of a 'varying' reference correlator. The other correlation technique is called

Correlation B and produces results which are representative of a 'fixed' reference correlator.

- **Correlation Methods - Varying Sample Delay Value (N_d)**

  Correlation A shows trackable autocorrelation peaks for periodic signals regardless of the correlation shift number. The peaks appear for delay values corresponding to multiples of the signal period. Figure 4.3 shows this result. Every autocorrelation peak is distinguishable and independent of the correlation shift number (i.e., arbitrary segment selection). Therefore, 'promising' potential when periodic signals are used.

  Correlation B shows trackable autocorrelation peaks for periodic signals regardless of which correlation window is selected. The peaks appear for all correlation shift numbers corresponding to a respective delay value (i.e., reference window number). The peaks also occur every signal period. Figure 4.7 shows this result. Every autocorrelation peak is distinguishable and independent of the reference window number (i.e., arbitrary segment selection). Therefore, 'promising' potential when periodic signals are used.

- **Correlation Methods - Varying Correlation Window Size (N_w)**

  Both Correlation A and Correlation B show that the magnitude of the autocorrelation peak is directly proportional to correlation window size. As the correlation window increases, so does the magnitude of the autocorrelation peak. The user may use any correlation window size as long as the results are meaningful. Figure 4.11 and Figure 4.12 show this result.

The simulations for signals other than the reference signal showed the same overall trend where a larger correlation window yielded larger autocorrelation peak magnitudes. Thus, the correlation window size was fixed for all subsequent analysis and only the correlation delay was varied. For this research, the correlation window sizes were selected to be large enough to give meaningful results.

5.1.2 Correlation Peak Identifiability of AM Radio.   Although not 100% conclusive, analysis of initial results indicate that the navigation potential of AM radio signals may be limited. These results are based on CPI and arbitrary segment selection. The variation of results are shown below. The dB-scale surface plots are the primary tool for making these conclusions.

- **AM Song Signal with Correlation-A**

  The dB-scale surface plot of the AM song signal using Correlation A is shown in Figure 4.15. The correlation peak only appears sporadically when $N_d = 0$. At N_d = 0, the magnitude of the autocorrelation peak varies and is clearly dependent on the correlation shift number. This inconsistent trend gives reason to believe that the AM song signal only has 'limited' potential for navigation using the 'varying' correlation method A. A distinguishable autocorrelation peak does not occur for every arbitrary segment selection.

- **AM Song Signal with Correlation-B**

  The dB-scale surface plot of the AM song signal using Correlation B is shown in Figure 4.18. In terms of navigation potential, the actual autocorrelation peak is difficult to identify because there are many peaks within 2.0 dB of each other. These relatively indistinguishable results give reason to believe that the AM song signal only has 'limited' potential for navigation using the 'fixed' correlation method B. An autocorrelation peak does occur for every arbitrary segment selection but it is not definitely distinguishable.

- **AM Voice Signal with Correlation-A**

  The dB-scale surface plot of the AM voice signal using Correlation A is shown in Figure 4.22. The correlation peak appears sporadically throughout the matrix. Multiple peaks give reason to believe that the AM voice signal only has 'limited' potential for navigation using the 'varying' correlation method A. A distinguishable autocorrelation peak does not occur for every arbitrary segment selection.

- **AM Voice Signal with Correlation-B**

  The dB-scale surface plot of the AM voice signal using Correlation B is shown in Figure 4.25. In terms of navigation potential, there are many peaks within 2.0 dB of each other making it difficult to identify the actual autocorrelation peak. This undistinguishable result gives reason to believe that the AM voice signal only has 'limited' potential for navigation using the 'fixed' correlation method B. One distinguishable autocorrelation peak does not occur for every arbitrary segment selection.

The CPI for both song and voice AM radio signals for the purpose of navigation has been shown to be limited when using either correlation method. In the real-world, AM stations carry mostly spoken programs while FM stations carry mostly music [2]. It would be interesting to see if real AM radio voice signals would have promising navigation potential using this correlation receiver model.

5.1.3 Correlation Peak Identifiability of FM Radio. The variation with the most promising navigation potential of FM radio signals are the results with the 'fixed' reference Correlation B. These results are based on CPI and arbitrary segment selection. The variation of results are shown below. The dB-scale surface plots are the primary tool for making these conclusions.

- **FM Song Signal with Correlation A**

  The dB-scale surface plot of the FM song signal using Correlation A is shown in Figure 4.29. The correlation peak appearing only when $N_d = 0$. And when $N_d = 0$, the magnitude of the autocorrelation peak varies and is now dependent on the correlation shift number. This gives reason to believe that the FM song signal only has 'limited' potential for navigation using the 'varying' correlation method A. A distinguishable autocorrelation peak does not occur for every arbitrary segment selection.

- **FM Song Signal with Correlation B**

  The dB-scale surface plot of the FM song signal using Correlation B is shown in Figure 4.32. In terms of navigation potential, there is a 5.0 dB difference between the peak and sidelobes which makes it easy to identify the autocorrelation peak. This definite result gives reason to believe that the FM song signal has 'promising' potential for navigation using the 'fixed' correlation method B. Every autocorrelation peak is distinguishable and independent of the reference window number (i.e., arbitrary segment selection).

- **FM Voice Signal with Correlation A**

  The dB-scale surface plot of the FM voice signal using Correlation A is shown in Figure 4.36. The correlation peak appearing only when $N_d = 0$. And when $N_d = 0$, the magnitude of the autocorrelation peak varies and is now dependent on the correlation shift number. This gives reason to believe that the FM voice signal only has 'limited' potential for navigation using the 'varying' correlation method A. A distinguishable autocorrelation peak does not occur for every arbitrary segment selection.

- **FM Voice Signal with Correlation B**

  The dB-scale surface plot of the FM voice signal using Correlation B is shown in Figure 4.39. In terms of navigation potential, there is at least a 5.0 dB difference between the peak and sidelobes which makes it easy to identify the autocorrelation peak. This positive result gives reason to believe that the FM song signal has 'promising' potential for navigation using the 'fixed' correlation method B. Every autocorrelation peak is distinguishable and independent of the reference window number (i.e., arbitrary segment selection).

The CPI for both song and voice FM radio signals for the purpose of navigation is promising when using the 'fixed' reference Correlation B. Correlation A seems to only provide promising navigation potential when the signal is periodic. Unfortunately, AM and FM radio signals generally do not possess periodic structure. In the

real-world, FM stations predominantly carry music programs while AM stations predominantly carry voice programs [2]. It would be interesting to see how the navigation potential of real FM radio signals depends on voice or song modulation when using 'fixed' reference Correlation B.

5.2 Future Work

This research focused exclusively on simulation and there many different opportunities to expand the research. A few possible areas for future work are recommended below.

- **TDOA Measurements**

  Due to time constraints, actual TDOA measurements were never taken in this research. So the next logical step is to develop TDOA algorithms that determine the accuracy and usefulness of navigating with AM and FM radio signals. A simulated model would first need to be designed before real data is used.

- **Integration with Universal Software Radio Peripheral (USRP)**

  The Air Force Institute of Technology now has access to the Universal Software Radio Peripheral (USRP) receiver. The USRP is designed to allow general purpose computers to function as high bandwidth software radios [6]. The basic concept is that the USRP can replace the frontend receiver model of this research and collect real data. The daughter-boards of the USRP act as the RF frontend while the mother-board performs at the IF or BB level. The next challenge is to determine what is actually output from the USRP receiver and determine how the data can be used in the correlator models in this research. The USRP will hopefully allow the user to collect real filtered-downconverted data. With this capability, the simulated results of this thesis could be verified, as well as additional determinations made on the CPI and navigation potential of real-world AM and FM radio signals.

- **Different Signal Types**

  The real-world has so many different types of information being broadcast via radio signals. Another possible area of work is determining if there is difference of CPI and navigation potential for different signal types, e.g., signals generated for different musical genre: jazz, pop, rap, classical, etc. This research looked briefly into the difference between song and voice but it would be interesting to see if there is a difference between different genres of music. Related work on passive radar seems to suggest that a difference will be revealed.

- **Different Environments**

  Ideally, if the user can successfully integrate the USRP receiver with the correlation-receiver model(s) considered here, it would be interesting to consider additional experimental variables. Not only could different signal types be used, as stated above, but the environments where the data is collected could be varied. The motivation of this research started with GPS not operating well indoors, in urban areas and in dense vegetation. It would be interesting to analyze data from these different environments and determine what impact, if any, it has on overall results.

Again, there are so many different ways to expand upon this research and further evaluate the CPI and navigation potential of AM and FM radio signals. It is exciting to think about what may emerge as the correlation receiver techniques considered herein are integrated with the USRP receiver hardware.

Appendix A. MATLAB Code for Correlation Methods

This appendix contains the Matlab® code used to simulate the two correlation methods.

Listing A.1:   'Varying' Correlation Method A. (appendix1/correlatorA.m)

```matlab
% Correlator A - 'Varying' Reference
% 'x' is the undelayed signal of interest
% 'Nd' is the number of samples for the delay
% 'Nw' is the number of samples in the correlation window
5 % 'delta_w' is the number of samples in the shift
% 'delta_t' is the time increment between samples
% 'corr_A' is the correlation output

function [corr_A] = correlatorA(x,Nd,Nw,delta_w,delta_t)
10
     [x_undelay,x_delay] = delayA(x, Nd);
     N = length(x_delay);
     prod = x_undelay.*x_delay;

15   lowDex = 1;
     highDex = Nw;
     i = 1;
     corr_A = [];

20   while highDex <= N

        corr_A(i) = sum(prod(lowDex:highDex))*delta_t;
        lowDex = lowDex + delta_w;
        highDex = highDex + delta_w;
25      i = i+1;
     end

  end
```

Listing A.2:   'Fixed' Correlation Method B. (appendix1/correlatorB.m)

```matlab
% Correlator B - 'Fixed' Reference
% 'x' is the undelayed signal of interest
% 'Nd' is the number of samples for the delay
% 'Nw' is the number of samples in the correlation window
5 % 'delta_w' is the number of samples in the shift
% 'delta_t' is the time increment between samples
% 'corr_B' is the correlation output

function [corr_B] = correlatorB(x, Nd, Nw, delta_w, delta_t)
10
    [x_undelay,x_delay] = delayB(x, Nd);

    offset = 0;
    reference = x_undelay(1+offset:Nw+offset);
15

    lowDex = 1;
    highDex = Nw;
    i = 1;
20
    while highDex <= length(x_delay)
        shift = x_delay(lowDex:highDex);
        corr_B(i) = sum(reference.*shift)*delta_t;
        lowDex = lowDex + delta_w;
25      highDex = highDex + delta_w;
        i = i+1;
    end

end
```

Bibliography

1. Adamy, D. *EW 101: A First Course in Electronic Warfare.* Artech House, Norwood, Massachusetts, 2001.

2. Centre, B.C. "FM and AM Radio Station Electromagnetic Field Emissions". *Proceedings of the 41st IEEE Vehicular Technology Conference*, 1:1–3, June 2003.

3. Cong, Li and Weihua Zhuang. "Hybrid TDOA/AOA Mobile User Location for Wideband CDMA Systems". *IEEE Transactions on Wireless Communications*, 1:439–447, July 2002.

4. Deng, P. and PZ. Fan. "An AOA Assisted AOA Positioning System". *Proceedings of the International Conference on Communication Technology*, 2:1501–1504, March 2000.

5. Eggert, Ryan J. *Evaluating the Navigation Potential of the National Television System Committee Broadcast Signal.* Thesis, Air Force Institute of Technology, 2950 Hobson Way, March 2004.

6. Ettus, Matt. "USRP User's and Developer's Guide". Ettus Research LLC, Febuary 2005. Available at matt@ettus.com.

7. Fisher, Kenneth A. *Signals to Navigate and Their Exploitation.* Ph.D. thesis, Graduate School of Engineering, Air Force Institute of Technology (AETC), Wright-Patterson AFB OH, December 2002.

8. Garnder, W.A. "Spectral Correlation of Modulated Signals, Part 1: Analog Modulation". *IEEE Transactions*, 584–594, November 1987.

9. Goebel, Greg. "Radio Navigation Systems". Vector Site, Febuary 2005. Available at http://www.vectorsite.net/ttwiza.html.

10. Kim, Bryan S. *Trilateration and Time Difference of Arrival.* Research, Air Force Institute of Technology, 2950 Hobson Way, June 2005.

11. Lewis, T.S. *Radio and Television Engineers' Reference Book.* George Newnes Limited, London, 1955.

12. Lewis, T.S. *Empire of the Air: The Men Who Made Radio.* HarperCollins, New York, 1991.

13. Miller, Mikel M. *Non-GPS Precision In-Door and Out-Door Navigation.* Research description, Air Force Institute of Technology, 2950 Hobson Way, December 2004.

14. Misra, P and P Enge. *Global Positioning System: Signals, Measurements, and Performance.* Ganga-Jamuna Press, Massachusetts, 2001.

15. Mitra, Sanjit K. *Digital Signal Processing, A Computer Based Approach.* McGraw-Hill, Massachusetts, 2001.

16. Prasad, Ramjee and Tero Ojanpera. "An Overview of CDMA Evolution Toward Wideband CDMA". *IEEE Communications Surveys*, 1(1):2–29, July 1998.

17. Salmasi, Allen and Klein S. Gilhousen. "On the System Design Aspects of CDMA Applied to Digital Cellular and Personal Communications Networks". *Proceedings of the 41st IEEE Vehicular Technology Conference*, 1:19–22, May 1991.

18. Sklar, Bernard. *Digital Communications*. Prentice Hall, New Jersey, 2001.

19. Temple, Michael A. *EENG 669: Digital Communications I*. Course notes, Air Force Institute of Technology, 2950 Hobson Way, January 2005.

20. Temple, Michael A. *EENG 673: Spread Spectrum Communications*. Course notes, Air Force Institute of Technology, 2950 Hobson Way, June 2005.

21. Temple, Michael A. *Position Estimation using Non-GPS Waveforms*. Course description, Air Force Institute of Technology, 2950 Hobson Way, March 2005.

22. Thomas, N.J., D.G.M. Cruickshank, and D.I. Lauernson. "Performance of a TDOA-AOA Hybrid Mobile Location System". *Second International Conference on 3G Mobile Communication Technologies*, 1:216–220, March 2001.

23. Wikipedia. *GEE*. Wikimedia Foundation Inc., Florida, 2006.

24. Wikipedia. *Loran*. Wikimedia Foundation Inc., Florida, 2006.

25. Wikipedia. *Lorenz*. Wikimedia Foundation Inc., Florida, 2006.

26. Wikipedia. *Radiodetermination*. Wikimedia Foundation Inc., Florida, 2006.

27. Wikipedia. *Radiolocation*. Wikimedia Foundation Inc., Florida, 2006.

28. Wikipedia. *Radionavigation*. Wikimedia Foundation Inc., Florida, 2006.

29. Wikipedia. *Trilateration*. Wikimedia Foundation Inc., Florida, 2006.

30. Wikipedia. *VHF Omnidirectional Range*. Wikimedia Foundation Inc., Florida, 2006.

31. Zhu, Liangxue and Jinkang Zhu. "A New Model and its Performance for TDOA Estimation". *IEEE Communications Surveys*, 1:2750–2753, March 2001.

REPORT DOCUMENTATION PAGE

Form Approved
OMB No. 0704–0188

1. REPORT DATE (DD–MM–YYYY)	2. REPORT TYPE	3. DATES COVERED (From — To)
23–03–2006	Master's Thesis	Sept 2004 — Mar 2006

4. TITLE AND SUBTITLE

EVALUATING THE CORRELATION CHARACTERISTICS
OF ARBITRARY AM AND FM RADIO SIGNALS
FOR THE PURPOSE OF NAVIGATION

5a. CONTRACT NUMBER

5b. GRANT NUMBER

5c. PROGRAM ELEMENT NUMBER

6. AUTHOR(S)

Bryan S. Kim, Second Lieutenant, USAF

5d. PROJECT NUMBER

5e. TASK NUMBER

5f. WORK UNIT NUMBER

7. PERFORMING ORGANIZATION NAME(S) AND ADDRESS(ES)

Air Force Institute of Technology
Graduate School of Engineering and Management (AFIT/EN)
2950 Hobson Way
WPAFB OH 45433-7765

8. PERFORMING ORGANIZATION REPORT NUMBER

AFIT/GE/ENG/06-28

9. SPONSORING / MONITORING AGENCY NAME(S) AND ADDRESS(ES)

AFRL/SNRP
Mikel M. Miller, PhD
Bldg. 620, NE Delivery Dock
2241 Avionics Circle
WP AFB, OH 45433-7301 (973) 255-6127 x4274
mikel.miller@wpafb.af.mil

10. SPONSOR/MONITOR'S ACRONYM(S)

11. SPONSOR/MONITOR'S REPORT NUMBER(S)

12. DISTRIBUTION / AVAILABILITY STATEMENT

Approval for public release; distribution is unlimited.

13. SUPPLEMENTARY NOTES

14. ABSTRACT

The Global Positioning System (GPS) provides position estimates on the Earth at anytime, anywhere and in any weather. However, to provide robust positioning, GPS requires an unobstructed path to satellite signals. As such, GPS performance generally degrades or becomes non-existent in environments such as large urban areas. This research investigates and analyzes the correlation characteristics of arbitrary AM and FM radio signals for the purpose of navigation. Simulations are conducted with different combinations of correlation methods ('fixed' or 'varying'), modulation types (AM or FM), and signal types (song or voice). Out of the eight different variations considered, only two provided promising results for the purpose of navigation. Both the FM voice and FM song signals exhibit distinct autocorrelation peaks (i.e., 5.0 dB peak-to-sidelobe ratios) using the 'fixed' reference correlation method. However, results for both FM signal types revealed limited potential for navigation when using the 'varying' reference correlation method. All the AM signals considered yielded relatively limited potential for navigation using either correlation method.

15. SUBJECT TERMS

correlation characteristics, AM radio, FM radio, navigation, correlation methods

16. SECURITY CLASSIFICATION OF:			17. LIMITATION OF ABSTRACT	18. NUMBER OF PAGES	19a. NAME OF RESPONSIBLE PERSON
a. REPORT	b. ABSTRACT	c. THIS PAGE			Dr. Michael A. Temple, AFIT/ENG
U	U	U	UU	104	19b. TELEPHONE NUMBER (include area code) (937) 255–3636, ext 4279

Standard Form 298 (Rev. 8–98)
Prescribed by ANSI Std. Z39.18